The nature and significance of the Faroe-Shetland Terrane: linking Archaean basement blocks across the North Atlantic

R.E. Holdsworth, A. Morton, D. Frei, A. Gerdes, R.A. Strachan, E. Dempsey, C. Warren, A. Whitham

PII: S0301-9268(18)30275-4
DOI: https://doi.org/10.1016/j.precamres.2018.12.004
Reference: PRECAM 5226

To appear in: *Precambrian Research*

Received Date: 18 May 2018
Revised Date: 5 December 2018
Accepted Date: 5 December 2018

Please cite this article as: R.E. Holdsworth, A. Morton, D. Frei, A. Gerdes, R.A. Strachan, E. Dempsey, C. Warren, A. Whitham, The nature and significance of the Faroe-Shetland Terrane: linking Archaean basement blocks across the North Atlantic, *Precambrian Research* (2018), doi: https://doi.org/10.1016/j.precamres.2018.12.004

The nature and significance of the Faroe-Shetland Terrane: linking Archaean basement blocks across the North Atlantic

Holdsworth, R.E.[1], Morton, A.[2], Frei, D.[3], Gerdes, A.[4], Strachan, R.A.[5], Dempsey, E.[6], Warren, C.[7] & Whitham, A.[8]

1 = Department of Earth Sciences, Durham University, Durham, DH1 3LE, UK
2 = HM Research, Giddanmu, St Ishmaels SA62 3TJ, UK and CASP, University of Cambridge, Madingley Rise, Cambridge CB3 0UD, UK.
3 = Department of Earth Sciences, University of the Western Cape, 7530 Bellville, Western Cape, South Africa.
4 = Goethe-Universität Frankfurt, Institut für Geowissenschaften, Petrologie und Geochemie, Altenhöferallee 1, 60438 Frankfurt am Main, Germany.
5 = School of Earth and Environmental Sciences, University of Portsmouth, Portsmouth, PO1 3QL, UK.
6 = School of Environmental Sciences, University of Hull, Hull, HU6 7RX, UK
7 = School of Environment, Earth and Ecosystem Sciences, The Open University, Walton Hall, Kents Hill, Milton Keynes MK7 6AA, UK.
8 = CASP, University of Cambridge, Madingley Rise, Cambridge CB3 0UD, UK.

Abstract: Core samples of the continental basement rocks that underlie the eastern Faroe-Shetland Basin (FSB) and its inshore margins west of Shetland reveal a suite of predominantly granodioritic to granitic orthogneisses (including TTG), together with lesser volumes of foliated granitoids and subordinate dioritic to mafic gneisses and amphibolites. A small area of lithologically similar gneisses also crops out onshore at North Roe/Uyea west of the Caledonian front in Shetland. In the core samples, coarse grained gneissose textures and mineralogies consistent with upper amphibolite facies metamorphism are overprinted by a weak, but ubiquitous, static greenschist facies retrogression. Later structures include widespread epidote-quartz veining, and local developments of mylonite, cataclasite, pseudotachylite and phyllonite. Regions associated with the Rona Ridge oil fields (e.g. Clair, Lancaster) also preserve extensive brittle fracturing and associated low temperature hydrothermal mineralization (quartz, adularia, calcite, pyrite/chalcopyrite) with significant fracture-hosted hydrocarbons. New and published U-Pb zircon analyses from the gneisses offshore give a relatively narrow range of Neoarchaean protolith ages (ca 2.7-2.8 Ga) spread over a geographic area of 60,000 km^2 west of Shetland. Detrital zircon data from overlying Triassic-Cretaceous sedimentary sequences in the FSB suggest an equivalent limited range of Neoarchaean source materials. Hf isotopic data indicate involvement of Palaeo- to Mesoarchaean crustal sources. Overall, our findings suggest that a major phase of Neoarchaean crustal formation and associated high grade metamorphism dominates basement rocks in the region. They are similar in age and lithology to the protoliths of the nearest onshore Lewisian Complex of NW Scotland (Rhiconich Terrane). However, they lack geochronological or textural evidence for the widespread Proterozoic Laxfordian events (ca 1.7-1.8 Ga) which are widespread in Scotland. This suggests that the Precambrian rocks west of Shetland – the Faroe-Shetland Terrane - can be correlated with the Archaean rocks of the

Central Greenland-Rae Craton and that a northern limit of Proterozoic reworking lies just offshore from the north coast of Scotland.

Keywords: Lewisian; Faroe-Shetland; Neoarchaean; Nagssugtoqidian; Laxfordian; U-Pb geochronology.

Introduction

The nature, age and affinities of the onshore continental basement terranes in the circum-North Atlantic region are now fairly well understood (e.g. Park 2005, Wheeler et al. 2010; Mason 2015 and references therein). In contrast, our knowledge of the basement in many of the intervening offshore areas is relatively sparse since relatively few wells have penetrated through the overlying Palaeozoic to Recent sedimentary cover sequences. Even in wells where core materials exist, these have commonly not been studied in any great detail. An improved understanding of the age and affinities of basement in offshore regions will allow better constraints on the likely locations of major tectonic and terrane boundaries across the North Atlantic. It also better constrains which onshore areas are best used as surface analogues along the continental margins to investigate the potential influences of basement inheritance on the structural development of the Atlantic margins.

In this paper, we present new lithological descriptions and the results of U-Pb and Lu-Hf zircon geochronological studies from a range of basement rocks sampled in offshore borehole cores taken in the region west of Shetland and north of Scotland and the Outer Hebrides. These data supplement a small amount of information provided by Ritchie et al. (2011), which was largely based on a more detailed unpublished report by Chambers et al. (2005).

Location and Regional Setting

Geophysical evidence and geological sampling from the seabed and borehole cores suggests that continental basement rocks underlie a large region north of Scotland and west of Shetland. Precambrian basement rocks are exposed onshore in Shetland and on small islands north of Scotland and west of Orkney (notably Foula, Sule Skerry, Stack Skerry, Rona, Sula Sgeir; Fig. 1; Ritchie et al. 2011). West of the Walls Boundary Fault, most of these rocks are assigned to the Lewisian Gneiss Complex (Fig. 1), although some in Shetland are thought to be of younger Moine or Dalradian (i.e. Neoproterozoic) affinities (Flinn 1985). Offshore, the affinities of the basement are less certain, although the rocks are generally viewed as being correlatives of the Lewisian. Two prominent elongate basement ridges known as the Rona Ridge and Solan Bank High are buried beneath mainly Mesozoic and younger sedimentary rocks and define the southeastern margin of the Faroe-Shetland Basin. They

trend NE-SW running from north of Shetland to the NW tip of Scotland and lie in the uplifted footwalls of Mesozoic normal faults. A basement ridge of this trend continues to the south forming the Outer Hebrides island chain (Fig. 1).

In Scotland, the Archaean-Palaeoproterozoic Lewisian Gneiss Complex forms the basement of the foreland of the Ordovician-Silurian Caledonide orogen (Fig. 1). The western limit of the orogen is defined by the easterly-dipping Moine Thrust (Fig. 1), although Neoarchaean basement inliers within the Caledonian hinterland have been broadly correlated with the Lewisian (Friend et al. 2008). The gneiss complex represents a fragment of Laurentian crust that was juxtaposed with the European plate during the Early Palaeozoic Caledonian orogenic cycle, and subsequently separated from North America during the late Mesozoic to early Cenozoic opening of the North Atlantic Ocean. It is dominated by orthogneisses, the protoliths of which were emplaced between ca. 3.1 Ga and ca. 2.7 Ga. They were then subject to high-grade metamorphism at 2.7 and 2.5 Ga, dyke intrusion at ca. 2.4 and 2.0 Ga, and variably intense Palaeoproterozoic reworking at ca. 1.8-1.7 Ga (e.g. Whitehouse 1993; Kinny and Friend 1997; Friend and Kinny 2001; Whitehouse and Bridgewater 2001; Kinny et al. 2005; Park 2005; Wheeler et al. 2010; Mason 2012, 2016; Goodenough et al. 2013; Davies and Heaman 2014; Crowley et al. 2015). This geological history has strong similarities to the Nagssugtoqidian belt of SE Greenland, and the two segments of crust are thought to have been contiguous prior to opening of the North Atlantic (Kalsbeek et al. 1993; Friend and Kinny 2001; Park 2005).

The Shetland Islands form the northernmost exposures of the Caledonide orogen in the British Isles (Fig. 1). A large part of Shetland is underlain by Neoproterozoic to Cambrian metasedimentary successions that were deformed and metamorphosed during the Caledonian orogeny (Flinn 1985; 1988). In northwest Shetland, the easterly-dipping Uyea Shear Zone in the North Roe-Uyea area is probably structurally analogous to the Moine Thrust (Fig. 1; Walker et al. 2016). A suite of granitic orthogneisses and metagabbros in its footwall have been correlated directly with the Lewisian Gneiss Complex (Pringle 1970; Flinn et al. 1979; Flinn 1985, 2009).

Isolated U-Pb zircon data obtained from basement gneisses from offshore boreholes north and west of Shetland give ages in the range 2.7-2.8 Ga and lack any evidence for Palaeoproterozoic (Laxfordian) reworking (Chambers et al. 2005). This led Ritchie et al. (2011) to tentatively suggest that the Lewisian-like basement rocks lying to the west of the Walls Boundary fault could be assigned to a single Neoarchaean domain they termed the 'Faroe-Shetland Block'. This block, they suggested, is located northward of the eastwards continuation of the Nagssugtoqidian belt through mainland Scotland.

The present study has looked in detail at over 70 thin sections of basement gneisses from the offshore region west of Shetland. Some are existing sections held by the BGS or the Clair Joint Venture Group, but many are new. The locations of all offshore borehole cores that contain basement referred to in the present paper are shown in Figure 1.

Lithologies and Contact Relationships

Basement rocks

The most detailed description of basement lithologies to date is given in Chambers et al. (2005), summarised in Ritchie et al. (2011). It covered material studied from 42 offshore boreholes from a wide region extending from west of Shetland southwards to the Stanton High (west of Mull) and offshore to Rockall. In addition to thin section descriptions of lithologies, these authors also carried out major and trace element geochemistry on all samples.

The basement rocks west of Shetland are dominated by quartzofeldspathic granodioritic orthogneisses, with subordinate units of more granitic, intermediate and mafic compositions. Most of these gneisses are thought to be of tonalitic-trondhjemitic-dioritic affinity, although this has been proven using strict geochemical criteria in only a small number of samples (Chambers et al. 2005). The rocks are mostly foliated and show evidence for amphibolite facies regional metamorphism variably overprinted by a weak, but persistent low-grade retrogression. Later fault rocks, including mylonites and pseudotachylytes, are locally preserved but are very minor constituents.

The most complete set of basement cores come from the sub-horizontal 206/7a-2 well drilled by Elf through the Clair basement ridge in a SE to NW direction (Fig. 2a). These basement rocks are described in more detail below as it is possible to see some of the contact relationships of the various constituent gneisses in the six more or less continuous ca 9-10 m core sections (Fig. 2b). Furthermore, they exhibit a range of lithologies that are highly representative of the region west of Shetland (e.g. Chambers et al. 2005; Ritchie et al. 2011). Where necessary, reference will be made to other cores in cases where other features have been observed that are not seen in 206/7a-2 – logs of these additional cores are shown in Figure 3. Core from 206/8-8 has been varnished, so some of the best images of lithology are taken from that core, together with 206/7a-2 in Figure 4.

Medium to coarse grained, grey granodioritic gneiss (Fig. 4a) forms ca 55% of the 60 m of core from 206/7a-2. Subordinate interlayered units include medium to coarse grained pink granitic gneiss (15%, Fig. 4b) and foliated coarse grained porphyritic granite (15%, Fig. 4c – see also 206/9-2, Fig. 3). The latter rock type occurs as sheets apparently subparallel to the gneissic layering in most cases, although a single discordant example in 206/7a-2 is associated with a local cm-scale high strain shear zone (Fig. 4d). Units of green mafic gneiss (10%) and grey dioritic gneiss (5%) are also present locally and are commonly either interlayered with the other gneisses, or occur as earlier foliated enclaves (Fig. 4e, see also 206/8-8, Fig. 3). About 20% of the gneisses comprise mm- to cm-scale interlayered units of the various lithologies described above (Fig. 2b). In a few sections of core, metre-scale folding of the gneissic layering is preserved (Fig. 4f).

In thin section, the gneisses are typically medium to coarse grained, with cuspate-lobate grain boundary textures between quartz, feldspar and variably retrogressed mafic minerals (amphiboles, pyroxenes) consistent with high temperature regional metamorphism (Fig. 5a, b; e.g. Passchier and Trouw 2005). Marginal myrmekites and perthitic textures are widely preserved in rocks with more granitic compositions and are again consistent with moderate to low intensity high temperature deformation (Simpson 1985). Lower temperature subgrain rotation recrystallization textures are only very weakly developed, as are local deformation lamellae and undulose extinction in quartz grains. Originally calcic plagioclase grains are ubiquitous, but now commonly have more albitic compositions and are either altered to sericite or seeded with numerous tiny grains of epidote/clinozoisite (Fig. 5c). Likewise, pyroxenes are usually only preserved as local relict grains and are partially to completely pseudomorphed by fine grained intergrown aggregates of chlorite $\pm$ green biotite $\pm$ colourless amphibole $\pm$ epidote $\pm$ equigranular quartz $\pm$ calcite, titanite and ore; chlorite and epidote often occur as distinctive overgrowing coronae (Fig. 5d).

Overall, the rocks preserve textural and mineralogical evidence for early amphibolite facies regional metamorphism, which has then been variably overprinted by low temperature greenschist facies retrogression and (mostly) very low intensity associated strains. Overall finite strains are low and there is no compelling evidence pointing to more than one phase of prograde amphibolite facies deformation and metamorphism. Chambers et al. (2005) suggested that the preservation of rare examples of coarse-grained, two-pyroxene assemblages indicated that metamorphism locally reached granulite facies. Fine to ultrafine grained epidote-quartz veins are locally common cross-cutting the gneisses (Fig. 5e), as are small (mm-to-cm thick) rare cross-cutting units of phyllonite (also seen in 206/12-1, Fig. 3), cataclasite and pseudotachylyte (e.g. 206/9-2, Fig. 3).

Cover sequences

The Rona Ridge and Solan Bank High basement ridges are overlain by diverse, but volumetrically limited Late Palaeozoic-Mesozoic cover sequences. The impersistence of these mainly fluviatile-lacustrine to shallow marine deposits seems to reflect the long-term persistence of the ridges, with many local unconformities developed (Ritchie et al. 2011; Stoker et al. 2018). Basement - cover unconformities are sampled directly in several cores (Fig. 3), e.g. 205/21-1A (Lancaster, basement overlain by Jurassic Rona Sandstone), 206/8-8 (Clair, basement overlain by Devonian Clair Group) and 206/12-1 (southern Clair Ridge, basement overlain by possible upper Cretaceous breccia conglomerate – see below). In all cases, there is very little evidence of deep weathering profiles developed in the basement rocks underlying these unconformities. Clasts of all basement host and early fault rock types – bar pseudotachylyte – are found within the oldest overlying cover sequence in 206/8-8 (Fig. 5f, Devonian Clair Group). Later fractures and veins – which occur in both basement and Devonian to Jurassic cover sequences - are associated with widespread sediment-filled

fractures, quartz-adularia-calcite-base metal sulphide mineralization and hydrocarbons (bitumen, oil). These features will be described in separate publications.

Sample Locations and Descriptions

The core materials examined here are conveniently subdivided into four geographic groups, here termed (from northeast to southwest): '*Victory*', '*Greater Clair'*, '*Lancaster*' and '*Sula Sgeir-Orkney'* (Table I; Fig. 1). From these sub-areas, 14 samples have been dated using U-Pb zircon geochronology, complementing the three dates previously obtained from the study area by Chambers et al. (2005). In addition, Lu-Hf isotopic analyses were undertaken on 9 of the 14 zircon samples.

Sula Sgeir-Orkney sub-area

Sample HM11705 comes from 13.00 m depth in BGS borehole 88/02. The succession encountered in this borehole was described by Chambers et al. (2005) as comprising quartzo-feldspathic schist cut by cataclasite bands. The analysed sample is a strongly deformed medium grained granitic rock comprising quartz, K-feldspar, plagioclase, biotite and hornblende with minor titanite, epidote, allanite, ore, clinozoisite, zircon and secondary chlorite (after biotite and hornblende). The foliation is defined by a strong shape-preferred elongation of quartz, feldspar and mafic minerals. It is cut by several foliation-parallel cataclasite bands and associated pseudotachylytes (Fig. 6a).

Samples HM11709 and HM11711 come from BGS seabed cores (59-04/85DM and 59-04/186DM, respectively). HM11709 is a granitic gneiss containing sericitised plagioclase, quartz, K-feldspar, chlorite, biotite and muscovite, together with relict garnet, which is now mostly altered to chlorite, biotite and plagioclase. HM11711 is a highly altered granite, consisting of quartz, sericitised plagioclase, epidote, calcite and clay minerals.

Lancaster sub-area

Sample HM11686 comes from exploration well 204/25-1 (depth 2870.43 m) and is a coarse grained interbanded unit of granodioritic-dioritic gneiss (Fig. 6b). It comprises varying proportions of plagioclase, quartz, green pyroxene and hornblende, ore minerals, secondary chlorite, and accessories (allanite, apatite, zircon). It is cut by small fractures with associated calcite veining.

Sample HM11687, from exploration well 204/26-1A (depth 2648.68 m), is a medium to coarse grained granodioritic gneiss. It comprises sericitized plagioclase, quartz and altered mafics (after amphibole or pyroxene), which are now mainly fine-grained chlorite, epidote and ore minerals. Apatite and zircon are accessory phases.

Sample HM11688 comes from exploration well 204/27-1 (depth 2136.20 m) and is a medium to coarse grained granitic gneiss comprising plagioclase, K-feldspar, quartz, biotite and titanite, with accessory ore, allanite and secondary chlorite. Other than fracturing, there is little evidence for low temperature overprinting in quartz grains.

Sample HM11689 comes from exploration well 204/28-1 (depth 1941.55 m) and is a granodioritic gneiss comprising sericitized plagioclase, quartz, K-feldspar, biotite and sparse grains of green amphibole, both of which are altered to secondary chlorite. Accessories include ore, allanite and zircon. Quartz grains show minor development of undulose extinction but otherwise preserve high temperature coarse grain sizes and cuspate-lobate boundaries with feldspars.

Greater Clair sub-area

Sample HM11691 comes from exploration well 205/20-1 (depth 2017.50 m) and is a coarse grained granitic gneiss. It comprises plagioclase, K-feldspar, quartz, brown-green hornblende, altered pyroxene, and accessories (ore, allanite, zircon, epidote, titanite, apatite). The rock is weakly foliated with well-developed marginal myrmekite development (Fig. 6c). Some minor subgrain development and fine subgrain rotation recrystallization is preserved in quartz with numerous microcracks filled with epidote.

Samples HM11692 and **HM11694** are both taken from exploration well 206/7a-2, at depths 2141.40 m and 2593.30 m respectively. They are medium to coarse grained granodioritic gneisses comprising plagioclase, quartz, K-feldspar and mafics (amphibole, biotite, chlorite – possibly after pyroxene), together with minor amounts of epidote, allanite, apatite, zircon, ore and titanite. Whilst dominated by coarse grained high temperature fabrics, mm-wide zones of low temperature brittle-ductile overprinting are evident and are associated with increased retrogression and breakdown of plagioclase to fine grained aligned aggregates of white mica and epidote (Fig. 6d). Associated quartz grains show evidence of limited marginal subgrain rotation recrystallization in these regions and feldspar clasts have fibrous quartz-white mica tails consistent with the operation of solution-precipitation creep (Fig. 6d).

Sample HM22702 is a coarse grained granodioritic gneiss from exploration well 206/12-1 (depth 1716.65 m). It comprises highly sericitised plagioclase, quartz and fine-grained aggregates of brown biotite together with accessory apatite, ore, epidote and zircon.

Victory Sub-area

Sample HM11698 comes from exploration well 208/23-1 (depth 2071.26 m) and is a granitic gneiss comprising plagioclase, K-feldspar, quartz and minor amounts of ore, epidote, titanite, limonite and zircon. It preserves evidence of moderate deformation at high temperatures with elongate quartz grains domains only locally overprinted by weak subgrain development and bulging recrystallization. Plagioclase is heavily saussuritized and is substantially replaced by fine calcite-quartz intergrowths.

Sample HM11699, from exploration well 208/26-1 (depth 3741.31 m), is a medium to coarse grained granodioritic gneiss containing plagioclase, quartz, brown biotite, brown-green hornblende, relict clinopyroxene (2%) and accessories (ore, epidote). Fine aggregates of green amphibole, biotite and epidote occur locally, possibly after orthopyroxene (Fig. 6e). Both hornblende and biotite are locally altered to fine aggregates of secondary chlorite. Cuspate-lobate quartz-feldspar grain boundaries are well developed with very little low temperature recrystallization of quartz.

Sample HM11700 comes from exploration well 208/27-2 (depth 1357.11 m) and is a mixture of coarse grained granitic and more mafic granitic gneiss. The mafic unit comprises plagioclase, K feldspar, quartz, brown partially altered pyroxene and accessories (ore, epidote, apatite, zircon) (Fig.

6f). The pyroxene is altered locally to blue-green amphibole and has prominent ore-rich alteration rims. The more leucocratic unit comprises plagioclase, K-feldspar and quartz with minor biotite and epidote.

U-Pb and Lu-Hf Zircon Geochronology

Analytical methods

The samples chosen for analysis (Table I) were collected from a larger sample set, some of which did not yield minerals suitable for U-Pb dating. Following thin-section preparation, the samples were crushed to < 250 μm at the Open University, Milton Keynes, UK. Zircons were concentrated using a combination of magnetic separation and heavy liquid treatment. The final separation step was made by hand-picking zircon grains from the heavy and non-magnetic fraction using an optical microscope. The individual zircon grains were mounted on double-sided, transparent adhesive tape and subsequently embedded in 1-inch diameter circular epoxy mounts for polishing.

All U-Pb age data were obtained at the Central Analytical Facility (CAF), Stellenbosch University, South Africa, by laser ablation - single collector - magnetic sectorfield - inductively coupled plasma - mass spectrometry (LA-SF-ICP-MS) employing a Thermo Finnigan Element2 mass spectrometer coupled to a NewWave UP213 laser ablation system. All age data presented here were obtained by single spot analyses with a spot diameter of 30 μm and a crater depth of approximately 15-20 μm, corresponding to an ablated zircon mass of approximately 150-200 ng. The methods employed for analysis and data processing are described in detail by Gerdes and Zeh (2006) and Frei and Gerdes (2009). For quality control, the Plešovice (Sláma et al. 2008) and M127 (Nasdala et al. 2008; Mattinson 2010) zircon reference materials were analyzed, and the results were consistently in good agreement with the published ID-TIMS ages. Full analytical details and the results for all quality control materials analysed are given in Table II. The calculation of concordia ages and plotting of concordia diagrams were performed using Isoplot/Ex 3.0 (Ludwig 2003). CL (cathodoluminescence) imaging of the zircon grains was undertaken at the CAF using a Zeiss Merlin SEM, with a beam current of 10 nA and a 15 mm working distance. Analyses used for age calculations were screened for inheritance based on textures as revealed by CL images and ^{207}Pb-^{206}Pb age determinations, and are based on analyses that are 99-101% concordant. For calculations of upper intercept ages, anchoring of regression lines was not employed.

Also included in the U-Pb zircon geochronology study are four sandstone samples ranging in age from Triassic to Cretaceous. The analytical protocol followed for the detrital zircon study is identical to that for the basement samples described above, except that the grain size fraction was that used routinely for conventional heavy mineral provenance investigations (63-125 μm).

Hafnium isotope measurements were performed with a Thermo-Finnigan NEPTUNE multi collector ICP-MS at Goethe University Frankfurt (GUF) coupled to RESOlution M50 193nm ArF Excimer (Resonetics) laser system following the method described in Gerdes and Zeh (2006, 2009). Between 10 and 19 individual zircons per sample were analysed. Prior to Hf-isotope analysis, the internal textures were investigated by cathodoluminesence imaging. Only homogeneous growth zones in zircons yielding concordant or nearly concordant U-Pb ages were targeted for Hf-isotope analysis. Spots of 40 µm in diameter were drilled with a repetition rate of 5.5 Hz and an energy density of 6 J/cm^2 during 50s of data acquisition. The instrumental mass bias for Hf isotopes was corrected using an exponential law and a $^{179}Hf/^{177}Hf$ value of 0.7325. In case of Yb isotopes, the mass bias was corrected using the Hf mass bias of the individual integration step multiplied by a daily βHf/βYb offset factor (Gerdes and Zeh 2009). All data were adjusted relative to the JMC475 of $^{176}Hf/^{177}Hf$ ratio = 0.282160 and quoted uncertainties are quadratic additions of the within run precision of each analysis and the reproducibility of the JMC475 (2SD = 0.0028%, n = 8). Accuracy and external reproducibility of the method was verified by repeated analyses of reference zircon GJ-1 and Plesovice, which yielded a $^{176}Hf/^{177}Hf$ of 0.282010 ± 0.000025 (2 SD, n=7) and 0.0282475 ± 0.000020 (n=7), respectively. This is in excellent agreement with previously published results (e.g. Gerdes and Zeh 2006; Slama et al. 2008) and with the LA-MC-ICPMS long-term average of GJ-1 (0.282010 ± 0.000025; n > 800) and Plesovice (0.282483 ± 0.000025, n > 300) reference zircon at GUF.

The initial $^{176}Hf/^{177}Hf$ values are expressed as εHf(t), which is calculated using:

(i) a decay constant value of 1.867×10^{-11} year^{-1}
(ii) CHUR after Bouvier et al. (2008; $^{176}Hf/^{177}Hf_{CHUR, today}$ = 0.282785 and $^{176}Lu/^{177}Hf_{CHUR, today}$ = 0.0336), and
(iii) the apparent Pb-Pb ages obtained for the respective domains.

For the calculation of Hf two stage model ages (T_{DM}) in billions of years, the measured $^{176}Lu/^{177}Hf$ of each spot (first stage = age of zircon), a value of 0.0113 for the average continental crust, and a depleted mantle $^{176}Lu/^{177}Lu$ DM = 0.0384 and $^{176}Hf/^{177}Hf$ DM = 0.283165 (average MORB; Chauvel et al. 2008) were used.

Results: U-Pb ages from basement rocks

The 14 samples of crystalline basement rocks dated here yield a comparatively limited range of zircon U-Pb ages within the Neoarchaean (Table III). These data lie in the same age range as the 3 dates obtained by Chambers et al. (2005) in the same study area, which are also listed in Table III.

Sula Sgeir-Orkney sub-area

Sample HM11705 (BGS borehole 88/02, 13.00 m) contains elongate prismatic zircons with typical oscillatory igneous zonation patterns (Figs 7a and b). Occasional zircons are strongly metamict, but nevertheless retain remnant oscillatory zoning (Fig. 7b). They display a discordant trend with an upper intercept age of 2754 ± 22 Ma with an MSWD of 0.88 (Fig. 8a).

Sample HM11709 (BGS seabed core 59-04/85DM) has equant to elongate prismatic zircons with indistinct oscillatory magmatic zoning. They are mostly dark under CL (high-U) with a small number of grains having bright rims. The main zircon group yields a concordia age of 2747 ± 7 Ma with an MSWD of 0.42 and a probability of concordance of 0.99 (Figs 8b and c). In addition, there is a small number of older zircons interpreted as inherited, together with two zircons with younger ages (2621 ± 26 Ma and 2628 ± 28 Ma) probably related to Pb-loss during a subsequent Neoarchaean thermal (possibly hydrothermal) event.

Sample HM11711 (BGS seabed core 59-04/186DM) has a zircon population with a concordia age of 2826 ± 5 Ma, with an MSWD of 0.45 and a probability of concordance of 1.00 (Figs 8d and e), excluding a single younger zircon dated as 2681 ± 39 Ma.

Lancaster sub-area

Sample HM11686 (204/25-1, 2870.43 m) contains equant to stubby subhedral to subrounded zircons that show evidence of resorbtion. Grains show indistinct oscillatorily-zoned centres that are dark under CL, with bright rims that also have magmatic textures (Fig. 7c). Many of the zircons in this sample are moderately to highly fractured. On the Wetherill concordia diagram, they show a discordant trend with an upper intercept age of 2729 ± 12 Ma with an MSWD of 0.52 (Figs 9a and 9b). In addition, there is an older less precise analysis at ca 2850 Ma, interpreted as inherited, and a small number of slightly younger zircons.

Sample HM11687 (204/26-1A, 2648.68 m) contains zircons with indistinct oscillatory magmatic zoning, with euhedral to subhedral relatively equant morphologies. They fall on a discordant trend (Figs 9c and 9d) with an upper intercept age of 2733 ± 14 Ma (MSWD = 2.0), but there is one older grain dated as ca. 3100 Ma, interpreted as inherited. The four zircons with 100% concordance yield a concordia age of 2744 ± 16 Ma with an MSWD of 0.41 and probability of concordance of 0.84 (Fig. 9e).

Sample HM11688 (204/27-1, 2136.20 m) has prismatic zircons that range from stubby to moderately elongate, and are euhedral to subrounded. Some display indistinct oscillatory magmatic zoning (Fig. 7d) but many show metamictisation/recrystallisation owing to relatively high U contents, which has partially or wholly destroyed the original igneous zoning fabric. They display a discordant trend (Figs 9f and g) with an upper intercept age of 2745 ± 15 Ma (MSWD = 4.2). The concordant zircons yield a concordia age of 2739 ± 8 Ma

with an MSWD of 0.87 and probability of concordance of 0.62 (Fig. 9h). As with sample HM11687, there is also evidence for a minor inherited component.

Sample HM11689 (204/28-1, 1941.55 m) has zircons that display a discordant trend (Fig. 9i) with an upper intercept age of 2762 ± 13 Ma (MSWD = 8.6). The concordant zircons yield a concordia age of 2793 ± 10 Ma with an MSWD of 1.0 and probability of concordance of 0.45 (Fig. 9j).

Greater Clair sub-area

Sample HM11691 (205/20-1, 2017.50 m) has equant to prismatic, euhedral, subhedral and subrounded zircons with typical igneous dark oscillatory zoning, many of which are surrounded by brighter oscillatorily-zoned rims that are also magmatic, produced by resorbtion in the melt (Figs 7e and f). In some cases (Fig. 7e), there is evidence for several phases of zircon growth and resorbtion. The zircons display a discordant trend (Fig. 10a) with an upper intercept age of 2736 ± 12 Ma (MSWD = 0.96). There is no significant difference in age between the dark grain centres and the brighter rims (Figs 7e and f).

Sample HM11692 (206/7a-2, 2141.40 m) has mostly elongate euhedral to subhedral zircons with relatively indistinct oscillatory magmatic zoning. Some of the zircons have bright oscillatorily-zoned rims that are also magmatic. When plotted on a Wetherill concordia diagram, the data reveal a degree of scatter along the concordia line, precluding determination of an upper intercept age (Fig. 10b). However, the main group of zircons yield a concordia age of 2806 ± 8 Ma with an MSWD of 0.41 and probability of concordance of 0.84 (Fig. 10c). There appears to be a subordinate younger cluster at ca 2750 Ma.

Sample HM11694 (206/7a-2, 2593.30 m) has zircons that display a discordant trend (Fig. 10d) and yield an upper intercept age of 2753 ± 14 Ma (MSWD = 1.6) (Fig. 10e).

Sample HM22702 (206/12-1, 1716.65 m) has mostly elongate prismatic euhedral to subhedral zircons with typical magmatic oscillatory zoning patterns (Fig. 7g). There is evidence for several phases of zircon growth with both dark and bright areas under CL, but there is no significant difference in age between the two. The data define a discordant trend with an upper intercept age of ca. 2748 Ma (Fig. 10f). There is some scatter in the ages determined from the sample, which extend back to 2828 Ma. This is interpreted as indicating the presence of inherited zircons and suggests a relatively prolonged history of basement formation and stabilisation.

Victory Sub-area

Sample HM11698 (208/23-1, 2071.26 m) has equant to prismatic euhedral to subhedral zircons with typical igneous dark oscillatory zoning, many of which are surrounded by brighter oscillatorily-zoned rims that are also magmatic. These textures indicate the zircons underwent partial resorbtion in the melt prior to a later stage of crystallisation, but there is

no significant difference in age between the dark grain centres and the brighter rims (Fig. 7h). The zircon data display a discordant trend (Fig. 10g) with an upper intercept age of 2776 ± 12 Ma (MSWD = 2.6).

Sample HM11699 (208/26-1, 3741.31 m) has zircons that are all close to concordia, but show significant scatter that precludes meaningful determination of an upper intercept age (Fig. 10h). The zircons have generally equant to stubby prismatic morphology and range from euhedral to subrounded. Many of the zircons are dark under CL with oscillatory magmatic zoning, but most of these have bright margins that display broad, mosaic-like textures that are typically of anatectic origin (Figs 7i and j). Other zircons are entirely bright under CL and show only anatectic textures. The probability density plot (Fig. 11a) shows the presence of two main groups, one in the 2720-2760 Ma range and one (possibly bimodal) in the 2800-2860 Ma range. This is the only sample in the data set that shows a significant difference in age between the dark cores and the bright rims (Fig. 7j), and the bimodal age distribution is believed to be a manifestation of at least two phases of zircon growth. The earlier phase (ca 2800-2860 Ma) generated zircons with typical oscillatory magmatic zoning that have dark CL (relatively high U), whereas the later phase (ca 2720-2760 Ma) generated zircons with anatectic textures, either as rims on the older grains or as entirely new grains.

Sample HM11700 (208/27-2, 1357 m) has zircons that are mostly concordant or near-concordant (Fig.10i), and yield a concordia age of 2789 ± 8 Ma with an MSWD of 0.76 and probability of concordance of 0.78 (Fig. 10j).

Results: U-Pb ages of detrital zircons in cover sequences

In addition to U-Pb zircon data that give direct measurement of basement ages, detrital zircon data may provide additional information. Four sandstone samples from the eastern part of the Faroe-Shetland Basin, ranging in age from Triassic to Early Cretaceous, have yielded almost exclusively Neoarchaean age spectra consistent with the data presented above. Three of these samples are located in reasonably close proximity to basement penetrations: HM12189 (204/27-1, 2094.65 m) and HM12194 (202/3-1A, 1642.50 m), which are located adjacent to the Lancaster sub-area, and HM12357 (206/4-1, 4115 m), which is close to the Greater Clair sub-area (Fig. 1). The other sample (HM12172, 213/23-1, 3598.36 m) has greater areal significance, since it is located further west in the basin, close to the Corona Ridge (Fig. 1), but it is nearest to the Victory sub-area.

<u>Lancaster sub-area</u>

Samples HM12189 (204/27-1, 2094.65 m) and HM12194 (202/3-1A, 1642.50 m) are both from sandstones of the Upper Jurassic Rona Member (Kimmeridge Clay Formation). The Rona sandstones were deposited by fan-deltas draining adjacent Archaean basement highs as a result of footwall uplift on normal faults bounding the Rona and Judd Highs (Fig 1; Verstralen et al. 1995). Both samples have detrital zircon populations that are overwhelmingly dominated by a 2680-2820 Ma group (Fig. 11b, c), consistent with local

basement sourcing, although the sample from 202/3-1a contains a small number of younger zircons ranging from Palaeoproterozoic to Early Palaeozoic, suggesting minor involvement of other source materials.

Greater Clair sub-area

Sample HM12357 is from the Lower Cretaceous Royal Sovereign Formation at 4115 m depth in well 206/4-1, located immediately to the northwest of the Clair Field area (Fig. 1). The zircon population is almost exclusively Archaean, dominated by a Neoarchaean group between 2660 Ma and 2780 Ma with three older zircons with scattered ages between 2940 Ma and 3040 Ma (Fig. 11d).

Well 213/23-1 (Victory sub-area)

Sample HM12172 is from a Triassic sandstone at 3598.36 m depth in well 213/23-1, located significantly further basin-ward compared with all other samples in the study. Excluding two younger zircons at 1096 Ma and 1751 Ma, the spectrum is exclusively Archaean. In this case, however, the distribution is polymodal, with three main groups being apparent. The largest group lies between 2760-2900 Ma, with smaller groups at 2640-2740 Ma and 2920-2980 Ma (Fig. 11e).

Results: Lu-Hf data from basement rocks

The εHf(t) versus U-Pb crystallisation age diagram (Fig. 12) suggests the presence of three distinct groups within the sample set. The two basement samples from the Victory sub-area (HM11698: 208/23-1, 2071.26 m and HM11700: 208/27-2, 1357.11 m) have depleted mantle model ages of 3200-3300 Ma. These data indicate recycling of older crustal components of probable Palaeoarchaean age (extracted from the depleted mantle at ca 3200 to 3300 Ma) during the formation of new crust at ca 2750 to 2800 Ma.

In contrast, basement samples HM11686 (204/25-1, 2870.43 m, Lancaster sub-area), HM11691 (205/20-1, 2017.50 m, Greater Clair sub-area) and HM11711 (59-04/186DM, Sula Sgeir-Orkney sub-area) have younger model ages indicating extraction from the depleted mantle at ca 2900 to 3000 Ma. Therefore, this group represents recycling of Mesoarchaean crust during crustal formation events at ca 2750 to 2800 Ma. Crystalline basement samples HM11694 (206/7a-2, 2593.30 m, Greater Clair sub-area) and HM11705 (88/02, 13.00 m, Sula Sgeir-Orkney sub-area) have intermediate model ages, indicating they originated through melting of crust extracted from the depleted mantle during the Palaeoarchaean to Mesoarchaean.

Discussion and conclusions

The 17 basement age determinations presented here fall in a relatively narrow range between 2729-2826 Ma, similar to the 2700-2829 Ma ages obtained from 3 samples in the same area by Chambers et al. (2005). The geographic distribution of the 20 ages obtained is shown in Figure 13 – there is no clear difference in age ranges in any of the 4 sub-areas defined here.

By contrast, Hf isotope data from the Neoarchaean samples indicate that despite the relatively limited range in their U-Pb crystallisation ages, there is evidence for significant variation in their pre-crystallisation history (Figs 12 and 13). Extraction from the depleted mantle varied in age from ca 3200 Ma to ca 2900 Ma. The oldest Hf T_{DM} ages are from the Victory sub-area (wells 208/23-1 and 208/27-2), which is the most northeasterly segment in the study. Therefore, although the data set is limited, there is evidence for lateral variations in the Hf model age data that may indicate the existence of different crustal domains in the Neoarchaean of the west of Shetland area.

The uniformity in U-Pb crystallization ages of basement is strikingly consistent with the restricted range of Neoarchaean sources seen in detrital zircons preserved in sediments from various stratigraphic levels and locations in cover sequences in the eastern part of the Faroe-Shetland Basin. These include the Upper Jurassic Rona Formation in 202/3-1a and 204/27-1 and the Lower Cretaceous Royal Sovereign Formation in 206/4-1. The Triassic of 213/23-1 records two events in a similar but somewhat wider range (2640-2900 Ma), together with an earlier event between 2920-2980 Ma. This earlier group partially overlaps with one of the main zircon components (ca 2960-3020 Ma) seen in Archaean-sourced Albian sandstones from Kangerlussuaq, East Greenland (Whitham et al. 2004). In none of the cases described above is there any evidence for Proterozoic reworking of Archaean crust.

It should be noted that the discordant arrays of data visible in some samples in Figures 9 and 10 trend downwards to mainly Mesozoic lower intercept ages. The significance of these is not completely understood at present, but they most likely reflect lead loss during thermal events associated with Phanerozoic basin development. Further investigations will be aimed at clarifying the low temperature history of the basement during Mesozoic rifting.

Neoarchaean events in the Faroe-Shetland basement rocks

The U-Pb zircon analyses of intermediate to felsic basement gneisses from offshore boreholes in the FST reported herein and by Chambers et al. (2005) reveal that the majority of ages range from 2829 Ma to 2700 Ma. The analysed grains are primarily magmatic with oscillatory zoning, and many show evidence of several phases of crystallisation. In most cases, there is no significant difference in age between the different growth phases, but in one sample there is clear evidence for two distinct events. A small number of samples contain older outliers, interpreted as inherited. In contrast to Chambers et al. (2005), we have found no compelling textural evidence within the zircon grains for granulite facies

metamorphism: the U-Pb ages are therefore believed to date the crystallisation of the igneous protoliths. The only clear example of complexity is seen in the zircons from 208/26-1, where the bimodal age distribution suggests at least two phases of zircon growth at ca 2800-2860 Ma and ca 2720-2760 Ma, with the latter group of zircons preserving evidence of anatectic textures, either as rims on the older grains or as entirely new grains.

The majority of the crystallisation ages fall between ca 2720 Ma and ca 2750 Ma, but show a bimodal distribution with a subordinate group between ca 2790 Ma and ca 2840 Ma (Fig. 14). It therefore appears that the Faroe-Shetland Terrane underwent a prolonged phase of stabilisation between ca 2840 Ma and 2700 Ma, with the main phase taking place between 2720-2750 Ma. From the presently-available data, there does not appear to be any geographic trend in the crystallisation ages (Fig. 13), although the detrital zircon data from well 213/23-1, further west than all the basement penetrations, indicates some older events, a picture that is also inferred from cover sediments in Kangerlussuaq on the conjugate margin (Whitham et al., 2004) (Fig. 11f).

Comparison with the Lewisian Gneiss Complex

The new data reported here provide a firmer basis for assessing the proposed correlation of the basement rocks west of Shetland with the Lewisian Gneiss Complex of mainland Scotland and the Outer Hebrides. The U-Pb ages obtained fall within, although mainly at the lower end of, the broad range of emplacement ages that have been established for different components of the Lewisian Gneiss Complex (ca 3135-2680 Ma; Wheeler et al. 2010 and references therein). Sm-Nd model ages obtained by Chambers et al. (2005) lie in the range 3300-2830 Ma and are similar to those obtained from the Lewisian Gneiss Complex (3000-2700 Ma; Whitehouse 1989, Corfu et al. 1993). The Hf isotope data reported here from zircons in the basement west of Shetland indicate extraction from the depleted mantle from ca 3300 Ma to ca 2900 Ma. The igneous protoliths of the two gneiss complexes were therefore both emplaced during the same protracted period of Palaeo- to Neoarchaean crustal growth in the North Atlantic region (e.g. Garde et al. 2000; Nutman et al. 2010; Tappe et al. 2011; Dyck et al. 2015).

The main difference between the two gneiss complexes is that the basement gneisses west of Shetland show no sign in the U-Pb zircon analyses of the ca 2500 Inverian and ca 1800-1700 Ma Laxfordian amphibolite to granulite facies events that have been documented from different parts of the Lewisian Gneiss Complex (e.g. Kinny et al. 2005; Wheeler et al. 2010, Mason 2015 and references therein). The prolonged crustal history associated with the onshore Lewisian Complex is also reflected in detrital zircon ages from sediment in Abhainn Caslavat, which is a stream draining Lewisian TTG gneisses of the Tarbert Terrane (Outer Hebrides). The zircons in this stream sample identify both the ca 2850-3100 Ma and ca 1675 Ma events identified in the Tarbert Terrane by Kinny et al. (2005), as well as a large group of zircons between ca 2550 Ma and ca. 2850 Ma (Morton et al. 2012).

Regional correlations with Greenland

It is widely believed that the Lewisian Gneiss Complex of mainland Scotland was continuous with the Nagssugtoqidian mobile belt of SE Greenland prior to opening of the North Atlantic Ocean (Fig. 15; Friend & Kinny 2001; Park 2005). They display a similar range of Meso- to Neoarchaean protolith and metamorphic ages and both were strongly reworked during the Palaeoproterozoic. In SE Greenland, the Nagssugtoqidian mobile belt is limited to the north by Archaean rocks of the Central Greenland-Rae Craton (Fig. 15; Nutman et al. 2008; Kolb 2014) which was a stable crustal block during the Palaeoproterozoic. Detrital zircons in Albian and Eocene sandstones from the Kangerlussuaq region of the Rae Craton indicate three Archaean tectonothermal events (ca 2700–2750 Ma, 2960-3020 Ma and 3180-3200 Ma), and no evidence for subsequent thermal reworking (Whitham et al. 2004). The absence of evidence for Palaeoproterozoic reworking of the basement west of Shetland suggests that the eastern continuation of the northern limit of Nagssugtoqidian deformation must run generally WNW-ESE close to the northern coastline of mainland Scotland (Fig. 15). The basement rocks forming the small islands of Sula Sgeir, North Rona, Sule Skerry and Stack Skerry (Walker 1931; Nisbet, 1961) all lie close to the projected terrane boundary. New work to determine the compositions, ages and affinities of these gneisses will help to better constrain the possible location and nature of this important crustal boundary.

Another Lewisian terrane?

The traditional view of the Lewisian Complex (following Sutton & Watson 1951) is of a single crustal block that underwent early Scourian high-grade tectonothermal events which were later divided into Badcallian and Inverian. These rocks were then intruded by Palaeoproterozoic mafic dykes (Scourie dykes) and were then heterogeneously reworked during a lower-grade Laxfordian event. A different interpretation was put forward by Friend & Kinny (2001) and Kinny et al. (2005) who subdivided the complex into many discrete terranes, characterised by different geochronological signatures that were thought to have been amalgamated during the Proterozoic. This prompted a resurgence of interest in the Lewisian Complex, although many workers have subsequently concluded that the number of terranes may in fact be relatively small (e.g. Park 2005; Mason 2012, 2015).

In many ways, the debate illustrates the problems in applying “upper crustal” concepts such as terranes to deep crustal rocks. To what extent do variations in protolith ages and/or timing and grade of metamorphic events reflect dissection and telescoping of heterogeneous crust as opposed to genuine accretion of terranes in the original Cordilleran sense? Notwithstanding this, the Lewisian Complex does incorporate Palaeoproterozoic volcanic arc material, accreted oceanic material, and preserves evidence for high-P metamorphism, all of which are indicative of the presence of at least one suture (e.g. Baba 1998; Park et al. 2001; Mason et al. 2004). Furthermore, the northernmost mainland terrane of Kinny et al. (2005), the Rhiconich Terrane (Fig. 13), is still regarded as being sufficiently different from the Lewisian rocks to the south of the bounding Laxford Shear

Zone to constitute a separate terrane (Goodenough et al. 2010). Thus, a terrane approach to the analysis of the Lewisian Complex is still justified.

There is at present insufficient geochemical and isotopic data to support a detailed comparison of the Faroe-Shetland basement with the Rhiconich Terrane. Clearly the main difference lies in the lack of significant Palaeoproterozoic reworking of the former crustal block. Any Nagssugtoqidian suture likely lies further south within the Lewisian Complex (Fig. 15; see Mason 2015 for details). As a working hypothesis, however, we suggest that the Faroe-Shetland basement should have formal terrane status, but without the implication that the boundary with the Rhiconich Terrane is necessarily an additional suture zone. We suggest that the "Faroe-Shetland Terrane" represents the eastwards continuation of the foreland to the Nagssugtoqidian orogen, in much the same way that the Hebridean Terrane (incorporating the Lewisian Complex) represents the foreland to the much younger Caledonian orogen east of the Moine Thrust Zone (Bluck et al. 1992).

Acknowledgements

We are grateful to BP and Sindri for supporting the U-Pb geochronological studies of basement and Triassic-Cretaceous sandstones in the Faroe-Shetland Basin, and to BGS for access to samples. Clair JVG also supported the analysis of the basement cores and we would like to particularly acknowledge the extensive help of Catherine Witt, Farkhad Sadikhov and Andrew Robertson (BP), Caroline Gill (Shell), and Andy Conway (formerly ConocoPhillips). Ian Chaplin is thanked for his excellent thin sectioning skills. Lydia-Marie Joubert and Madelaine Frazenburg (CAF, Stellenbosch University) are thanked for their help with CL imaging. Editor Randy Parrish and reviewers Ian Millar and Anonymous are thanked for their very positive and constructive comments.

REFERENCES

Baba, S. 1998. Proterozoic anticlockwise P–T path of the Lewisian Complex of South Harris, Outer Hebrides, NW Scotland. Journal of Metamorphic Geology, 16, 819-41.

Bluck, B.J., Gibbons, W. and Ingham, J.K. 1992. Terranes. In: Cope, J.C.W.Ingham, J.K. and Rawson, P.F. (eds), Atlas of palaeogeography and lithofacies. Memoir of the Geological Society, London, 13, 1-4.

Bouvier, A., Vervoort, J. and Patchett, P. 2008. The Lu–Hf and Sm–Nd isotopic composition of CHUR: constraints from unequilibrated chondrites and implications for the bulk composition of terrestrial planets. Earth and Planetary Science Letters, 273, 48-57.

Chambers, L., Darbyshire, F., Noble, S. and Ritchie, D. 2005. NW UK continental margin: chronology and isotope geochemistry. British Geological Survey Commissioned Report, CR/05/095.

Chauvel, C., Lewin, E., Carpentier, M., Arndt, N. T. and Marini, J. 2008. Role of recycled oceanic basalt and sediment in generating the Hf–Nd mantle array. Nature Geoscience, 1, 64-67.

Corfu, F., Heaman L.M. and Rogers, G. 1994. Polymetamorphic evolution of the Lewisian complex, NW Scotland, as recorded by U-Pb isotopic compositions of zircon, titanite and rutile. Contributions to Mineralogy and Petrology, 117, 215-228.

Crowley, Q.C., Key, R. and Noble, S.R. 2015. High-precision U-Pb dating of complex zircon from the Lewisian Gneiss Complex of Scotland using an incremental CA-ID-TIMS approach. Gondwana Research, 27, 1381-1391.

Davies, J.H.F.L. and Heaman, L.M. 2014. New U-Pb baddeleyite and zircon ages for the Scourie dyke swarm: a long-lived large igneous province with implications for the Palaeoproterozoic evolution of NW Scotland. Precambrian Research, 249, 180-198.

Dyck, B., Reno, B.L. and Kokfelt, T.F. 2015. The Majorqaq Belt: A record of Neoarchaean orogenesis during final assembly of the North Atlantic Craton, southern West Greenland. Lithos, 220, 253-271.

Flinn, D. 1985. The Caledonides of Shetland. In: Gee, D.G. and Sturt, B.A. (eds), The Caledonide Orogen: Scandinavia and Related Areas. Wiley & Sons, New York, 1159-1172.

Flinn, D. 1988. The Moine rocks of Shetland. In: Winchester, J.A. (ed.), Later Proterozoic Stratigraphy of the Northern Atlantic Regions. Blackie, Glasgow, 74-85.

Flinn, D. 2009. Uyea to North Roe Coast. Lewisian, Torridonian and Moine Rocks of Scotland. Geological Conservation Review Series, 34, Joint Nature Conservation Committee, Peterborough, 628-634.

Flinn, D., Frank, P.L., Brook, M. and Pringle, I.R. 1979. Basement-cover relations in Shetland. In: Harris, A.L., Holland, C.H. and Leake, B.E. (eds) The Caledonides of the British Isles - Reviewed. Geological Society, London, Special Publications, 8, 109-115.

Frei, D. and Gerdes, A. 2009. Precise and accurate in-situ U-Pb dating of zircon with high sample throughput by automated LA-SF-ICP-MS. Chemical Geology, 261, 261-270.

Friend, C.R.L. and Kinny, P.D. 2001. A reappraisal of the Lewisian Gneiss Complex: geochronological evidence for its tectonic assembly from disparate terranes in the Proterozoic. Contributions to Mineralogy and Petrology, 142, 198-218.

Friend, C.R.L., Strachan, R.A. and Kinny, P.D. 2008. U-Pb zircon dating of basement inliers within the Moine Supergroup, Scottish Caledonides: implications of Archaean protolith ages. Journal of the Geological Society, London, 165, 807-815.

Garde, A.A., Friend, C.R.L., Nutman, A.P. and Marker, M. 2000. Rapid maturation and stabilisation of middle Archaean continental crust: the Akia terrane, southern West Greenland. Bulletin of the Geological Society of Denmark, 47, 1-27.

Gerdes, A. and Zeh, A. 2006. Combined U–Pb and Hf isotope LA-(MC-)ICP-MS analyses of detrital zircons: Comparison with SHRIMP and new constraints for the provenance and age of an Armorican metasediment in Central Germany. Earth and Planetary Science Letters, 249, 47-61.

Gerdes, A. and Zeh, A. 2009. Zircon formation versus zircon alteration - new insights from combined U–Pb and Lu–Hf in-situ LA-ICP-MS analyses, and consequences for the interpretation of Archean zircon from the Central Zone of the Limpopo Belt. Chemical Geology, 261, 230-243.

Goodenough, K.M., Park, R.G., Krabbendam, M., Myers, J.S., Wheeler, J., Loughlin, S.C., Crowley, Q.G., Friend, C.R.L., Beach, A., Kinny, P.D. and Graham, R.H. 2010. The Laxford Shear Zone: an end-Archaean terrane boundary? In: Law, R.D., Butler, R.W.H., Holdsworth, R.E., Krabbendam, M., Strachan, R.A. (Eds.), Continental Tectonics and Mountain Building : The Legacy of Peach and Horne, Geological Society, London, Special Publications, 335, 103-120.

Goodenough, K.M., Crowley, Q.C., Krabbendam, M. and Parry, S.F. 2013. New U-Pb age constraints for the Laxford Shear Zone, NW Scotland: evidence for tectonomagmatic processes associated with the formation of a Palaeoproterozoic supercontinent. Precambrian Research, 233, 1-19.

Jackson, S., Pearson, N.J., Griffin, W.L. and Belousova, E.A. 2004. The application of laser ablation – inductively coupled plasma – mass spectrometry to in situ U–Pb zircon geochronology. Chemical Geology, 211, 47-69.

Kalsbeek, F., Austrheim, H., Bridgwater, D., Hansen, B.T., Pedersen, S., Taylor, P.N. 1993. Geochronology of Archaean and Proterozoic events in the Ammassalik area, South-East Greenland, and comparisons with the Lewisian of Scotland and the Nagssugtoquidian of West Greenland. Precambrian Research 62, 239–270.

Kinny, P.D. and Friend, C.R.L. 1997. U-Pb isotopic evidence for the accretion of different crustal blocks to form the Lewisian Complex of northwest Scotland. Contributions to Mineralogy and Petrology, 129, 326-340.

Kinny, P.D., Friend, C.R.L. and Love, G.J. 2005. Proposal for a terrane-based nomenclature for the Lewisian Gneiss Complex of NW Scotland. Journal of the Geological Society, London, 162, 175-186.

Kolb, J. 2014. Structure of the Palaeoproterozoic Nagssugtoqidian Orogen, South-East Greenland: model for the tectonic evolution. Precambrian Research 255, 809-822.

Ludwig, K. 2003. Isoplot/Ex version 3: a Geochronological toolkit for Microsoft Excel. Geochronology Center, Berkeley, USA.

Mason, A.J. 2012. Major early thrusting as a control on the Palaeoproterozoic evolution of the Lewisian Complex: evidence from the Outer Hebrides, NW Scotland. Journal of the Geological Society, London, 169, 201-212.

Mason, A.J. 2015. The Palaeoproterozoic anatomy of the Lewisian Complex, NW Scotland: evidence for two 'Laxfordian' tectonothermal cycles. Journal of the Geological Society, 173, 153-169, https://doi.org/10.1144/jgs2015-026

Mason, A.J., Temperley, S. and Parrish, R.R. 2004. New light on the construction, evolution and correlation of the Langavat Belt (Lewisian Complex), Outer Hebrides, Scotland: field, petrographic and geochronological evidence for an early Proterozoic imbricate zone. Journal of the Geological Society, London, 161, 837-848.

Mattinson, J.M. 2010. Analysis of the relative decay constants of ^{235}U and ^{238}U by multi-step CA-TIMS measurements of closed-system natural zircon samples. Chemical Geology, 275, 186-198.

Morton, A., Ellis, D., Fanning, M., Jolley, D. and Whitham, A. 2012. Heavy mineral constraints on Paleocene sand transport routes in the Faroe-Shetland Basin. In: Varming, T. and Ziska, H. (eds), Faroe Islands Exploration Conference: Proceedings of the 3rd Conference. Annales Societatis Scientiarum Faeroensis, 56, 59-83.

Nasdala, L., Hofmeister, W., Norberg, N., Mattinson, J.M., Corfu, F., Dörr, W., Kamo, S.L., Kennedy, A.K., Kronz, A., Reiners, P.W., Frei, D., Košler, J., Wan, Y., Götze, J., Häger, T., Kröner, A. and Valley, J.W. 2008. Zircon M257 – a homogeneous natural reference material for the ion microprobe U-Pb analysis of zircon. Geostandards and Geoanalytical Research, 32, 247-265.

Nisbet, H. C. 1961. The geology of North Rona. Transactions of the Geological Society of Glasgow, 24, 169-189.

Nutman, A.P., Kalsbeek, F. and Friend, C.R.L. 2008. The Nagssugtoqidian orogen in South-West Greenland: evidence for Palaeoproterozoic collision and plate assembly. American Journal of Science, 308, 529-572.

Nutman, A.P., Friend, C.R.L. and Heiss, J. 2010. Setting of the c. 2560 Qôrqut Granite complex in the Archaean crustal evolution of southern West Greenland. American Journal of Science, 310, 1081-1114.

Park, R.G. 2005. The Lewisian terrane model: a review. Scottish Journal of Geology, 41, 105-118.

Park, R.G., Tarney, J. and Connelly, J.N. 2001. The loch Maree Group: Palaeoproterozoic subduction-accretion complex in the Lewisian of NW Scotland. Precambrian Research, 105,205-226.

Passchier, C.W. and Trouw, R.A.J. 2005. Microtectonics (Second edition) Springer, Berlin.

Pringle, I.R. 1970. The structural geology of the North Roe area of Shetland. Geological Journal. 7, 147-170.

Ritchie, J.D., Noble, D., Darbyshire, F., Millar, I. and Chambers, L., 2011. Pre-Devonian. In: Ritchie, J.D., Ziska, H., Johnson, H. and Evans, D. (eds), Geology of the Faroe-Shetland Basin and adjacent areas. BGS Research Report RR/11/01, 71-78.

Simpson, C. 1985. Deformation of granitic rocks across the brittle-ductile transition. Journal of Structural Geology. 7, 503-11.

Sláma, J., Košler, J., Condon, D.J., Crowley, J.L., Gerdes, A., Hanchar, J.M., Horstwood, M.S.A., Morris, G.A., Nasdala, L., Norberg, N., Schaltegger, U., Schoene, B., Tubrett, M.N. and Whitehouse, M.J. 2008. Plešovice zircon - a new natural reference material for U-Pb and Hf isotopic microanalysis. Chemical Geology, 249, 1-35.

Stacey, J.S. and Kramers, J.D. 1975. Approximation of terrestrial lead isotope evolution by a two-stage model. Earth and Planetary Science Letters, 26, 207-221.

Stoker, M., Holford, S.P. and Hillis, R.R. 2018. A rift-to-drift record of vertical crustal motions in the Faroe–Shetland Basin, NW European margin: establishing constraints on NE Atlantic evolution. Journal of the Geological Society, 175, http://dx.doi.org/10.1144/jgs2017-076

Sutton J. and Watson J. 1951. The pre-Torridonian metamorphic history of the Loch Torridon and Scourie areas in the north-west Highlands, and its bearing on the chronological classification of the Lewisian. Quarterly Journal of the Geological Society, London, 106, 241-307.

Tappe, S., Smart, K.A., Pearson, D.G., Steenfelt, A. and Simonetti, A. 2011. Craton formation in Late Archaean subduction zones revealed by first Greenland eclogites. Geology, 39, 1103-1106.

Walker, F. 1931. The Geology of Skerryvore, Dubh Artach, and Sule Skerry. Geological Magazine, 68, 315-323.

Walker, S., Thirlwall, M.F., Strachan, R.A. and Bird, A.F. 2016. Evidence from Rb-Sr mineral ages for multiple orogenic events in Caledonides of the Shetland Islands, Scotland. Journal of the Geological Society, London, 173, 489-503.

Wheeler, J., Park, R.G., Rollinson, H.R. and Beach, A. 2010. The Lewisian Complex: insights into deep crustal evolution. In: Law, R.D., Butler, R.W.H., Holdsworth, R.E., Krabbendam, M. and Strachan, R.A. (eds), Continental Tectonics and Mountain Building: The Legacy of Peach and Horne. Geological Society, London, Special Publications, 335, 51-79.

Whitehouse, M.J. 1989. Sm-Nd evidence for diachronous crustal accretion in the Lewisian Complex of Northwest Scotland. In: Ashwal, L.D. (ed.), Growth of the Continental Crust. Tectonophysics, 161, 245-256.

Whitehouse, M.J. 1993. Age of the Corodale gneisses, South Uist. Scottish Journal of Geology, 29, 1-7.

Whitehouse, M.J. and Bridgewater, D. 2001. Geochronological constraints on Palaeoproterozoic crustal evolution and regional correlations of the northern Outer Hebridean Lewisian complex. Precambrian Research, 105, 227-245.

Whitham, A.G., Morton, A.C. and Fanning, C.M. 2004. Insights into Cretaceous–Palaeogene sediment transport paths and basin evolution in the North Atlantic from a heavy mineral study of sandstones from southern East Greenland. Petroleum Geoscience, 10, 61-72.

Verstralen, I., Hartley, A. and Hurst, A. 1995. The sedimentological record of a late Jurassic transgression: Rona Member (Kimmeridge Clay Formation equivalent), West Shetland Basin, UKCS. In: Hartley, A. J. and Prosser, D. J. (eds), Characterization of Deep Marine Clastic Systems. Geological Society, Special Publications, 94, 155-176.

Tables

Table I) *Basement samples from offshore west of Shetland included in the currrent U-Pb isotopic analysis study. Locations are shown in Fig. 1.*

Sample number	Site	Long deg	Long min	Lat deg	Lat min	Company	Site type	Sample Depth (m)	Lithology
SULA SGEIR-ORKNEY									
HM11705	88/02	59	12.54	6	18.10	BGS	Shallow bh	13.00	Granitic gneiss
HM11709	59-04/85DM	59	37.68	3	21.84	BGS	Seabed core		Granodioritic gneiss
HM11711	59-04/186DM	59	42.30	3	30.04	BGS	Seabed core		Granite
LANCASTER									
HM11686	204/25-1	60	10.42	4	2.17	Hess	Expl well	2870.43	Granodioritic-tonalitic gneiss
HM11687	204/26-1A	60	9.29	4	53.25	Hess	Expl well	2648.68	Granodioritic gneiss
HM11688	204/27-1	60	9.54	4	39.17	BP	Expl well	2136.20	Granite
HM11689	204/28-1	60	9.49	4	32.01	BP	Expl well	1941.55	Granodioritic gneiss
GREATER CLAIR									
HM11691	205/20-1	60	27.39	3	7.01	Total	Expl well	2017.50	Granitic gneiss
HM11692	206/7a-2	60	41.16	2	36.43	Total	Expl well	2141.40	Granodioritic gneiss
HM11694	206/7a-2	60	41.16	2	36.43	Total	Expl well	2593.30	Granodioritic gneiss
HM22702	206/12-1	60	59.77	2	76.72	Shell	Expl well	1716.63	Granodioritic gneiss
VICTORY									
HM11698	208/23-1	61	10.14	1	30.55	Lasmo	Expl well	2071.26	Granitic gneiss
HM11699	208/26-1	61	7.05	1	49.15	BP	Expl well	3741.31	Granodioritic gneiss
HM11700	208/27-2	61	8.04	1	38.50	BP	Expl well	1357.11	Mafic-granitic gneiss

Table II) *LA-SF-ICP-MS U-Th-Pb dating methodology at CAF, Stellenbosch University*

Laboratory & Sample Preparation	
Laboratory name	Central Analytical Facility, Stellenbosch University
Sample type / mineral	Magmatic and detrital zircons
Sample preparation	Conventional mineral separation, 1 inch resin mount, 1 µm polish to finish
Imaging	CL, LEO 1430 VP, 10 nA, 15 mm working distance
Laser ablation system	
Make, Model & type	ESI/New Wave Research, UP213, Nd:YAG
Ablation cell & volume	Custom build low volume cell, volume ca.3 cm^3
Laser wavelength	213 nm
Pulse width	3 ns
Fluence	2.5 J/cm^{-2}
Repetition rate	10 Hz
Spot size	30 µm
Sampling mode / pattern	30 µm single spot analyses
Carrier gas	100% He, Ar make-up gas combined using a T-connector close to sample cell
Pre-ablation laser warm-up (background collection)	40 seconds
Ablation duration	20 seconds
Wash-out delay	30 seconds
Cell carrier gas flow	0.3 l/min He
ICP-MS Instrument	
Make, Model & type	Thermo Finnigan Element2 single collector HR-SF-ICP-MS
Sample introduction	Via conventional tubing
RF power	1100 W
Make-up gas flow	1.0 l/min Ar
Detection system	Single collector secondary electron multiplier
Masses measured	202, 204, 206, 207, 208, 232, 233, 235, 238
Integration time per peak	4 ms
Total integration time per reading	Approx. 1 sec
Sensitivity	20000 cps/ppm Pb
Dead time	16 ns
Data Processing	
Gas blank	40 second on-peak
Calibration strategy	GJ-1 used as primary reference material, Plešovice and M127 used as secondary reference material (Quality Control)
Reference Material info	M127 (Nasdala et al. 2008; Mattinson 2010); Plešovice (Slama et al. 2008); GJ-1 (Jackson et al. 2004)
Data processing package used / Correction for LIEF	In-house spreadsheet data processing using intercept method for laser induced elemental fractionation (LIEF) correction
Mass discrimination	Standard-sample bracketing with $^{207}Pb/^{206}Pb$ and $^{206}Pb/^{238}U$ normalised to reference material GJ-1
Common-Pb correction, composition and uncertainty	204-method, Stacey and Kramers (1975) composition at the projected age of the mineral, 5% uncertainty assigned
Uncertainty level & propagation	Ages are quoted at 2 sigma absolute, propagation is by quadratic addition. Reproducibility and age uncertainty of reference material and common-Pb composition uncertainty are propagated.
Quality control / Validation	Plešovice: Wtd ave $^{206}Pb/^{238}U$ age = 337 ± 4 (2SD, MSWD = 0.2) M127: Wtd ave $^{206}Pb/^{238}U$ age = 520 ± 5 (2SD, MSWD = 0.8)
Other information	Detailed method description reported by Frei and Gerdes (2009)

***Table III**) U-Pb ages of crystalline basement samples from the Hebridean margin.*
[1] Upper intercept U-Pb zircon age, this study. [2] Concordia U-Pb zircon age, this study. [3] Inferred U-Pb zircon age, this study. [4] Upper intercept U-Pb zircon age from Chambers et al. (2005) and Ritchie et al. (2011), obtained by ID-TIMS.

Sample number	Site	Lithology	U-Pb age (Ma)
'SULA SGEIR-ORKNEY'			
HM11705	88/02, 13.00 m	Granitic gneiss	2754 ± 22[1]
HM11709	59-04/85DM	Granodioritic gneiss	2747 ± 7[2]
HM11711	59-04/186DM	Granite	2826 ± 5[2]
'LANCASTER'			
	202/2-1, 1219.8 m	Quartzofeldspathic gneiss	2829 ± 46[4]
HM11686	204/25-1, 2870.43 m	Granodioritic-tonalitic gneiss	2729 ± 12[1]
HM11687	204/26-1A, 2648.68 m	Granodioritic gneiss	2733 ± 14[1], 2744 ± 16[2]
HM11688	204/27-1, 2136.20 m	Granite	2745 ± 15[1], 2739 ± 8[2]
HM11689	204/28-1, 1941.55 m	Granodioritic gneiss	2762 ± 13[1], 2793 ± 10[2]
	205/22-1, 3225.5 m	Dioritic gneiss	2700 ± 13[4]
GREATER CLAIR'			
HM11691	205/20-1, 2017.50 m	Granitic gneiss	2736 ± 12[1]
HM11692	206/7a-2, 2141.40 m	Granodioritic gneiss	2806 ± 8[2]
HM11694	206/7a-2, 2593.30 m	Granodioritic gneiss	2753 ± 14[1]
HM22702	206/12-1, 1716.63 m	Granodioritic gneiss	2748 ± 6[1]
	206/8-1A, 2310.9 m	Dioritic gneiss	2801.7 + 5.1/-4.6[4]
'VICTORY'			
HM11698	208/23-1, 2071.26 m	Granitic gneiss	2776 ± 12[1]
HM11699	208/26-1, 3741.31 m	Granodioritic gneiss	ca 2720-2760, ca 2800-2860[3]
HM11700	208/27-2, 1357.11 m	Mafic-granitic gneiss	2789 ± 8[2]

Figures

Figure 1) Map showing basement distribution at seabed, structural elements (grey lines) and drilled occurrences of basement (red dots, with well numbers) and cover sedimentary rocks (yellow dots) offshore that are referred to in the current paper; a combined red/yellow dot means that both basement and cover were studied. Boxes show location of sub-areas whilst inset map shows map of main structural features. WBF=Walls Boundary Fault; MTZ = Moine Thrust Zone, NRU = North Roe/Uyea area, Shetland, SSK = Sule Skerry, SST = Sule Stack, NR = North Rona, SSG = Sula Sgeir

Figure 2) Location and lithologies of borehole cores from the Clair Ridge. a) location map and interpreted seismic reflection profile through the basement ridge showing location of the sub-horizontal 206/7a-2 well and core sections (numbered). b) Logs of basement cores showing lithologies, contact relationships, locations of main cross-cutting faults and radiometrically dated samples (blue dots).

Figure 3) Location and lithologies of borehole cores from other key borehole cores. a) location map showing locations of borehole cores shown here. b) Logs of basement cores – and in 3 cases overlying cover rocks - showing lithologies, contact relationships and locations of early fault rock types.

Figure 4) Representative core specimens of typical basement lithologies. A) granodioritic gneiss; b) granitic gneiss; c) porphyritic granite; d) fold in gneisses cut by shear zone (SZ) that host a porphyritic granite sheet (see Fig 2b, Core 6); e) foliated dioritic gneiss enclave hosted in granitic gneiss; f) metre-scale folding of gneisses. Core and depths shown in all cases. Note that the prevalence of samples from 206/8-8 is due to this core having been slabbed and polished.

Figure 5) Typical mineralogy and textures seen in basement cores, with core and depths shown for each sample. a) Cross-polars view of typical granodioritic gneiss with cuspate-lobate quartz-feldspar contacts and irregular undulose extinction in quartz. b) PPL view of typical cuspate-lobate mafics-feldspar contacts, with late alteration of mafics (?originally pyroxene) to fine grained amphibole and chlorite, and feldspars to sericite. c) Higher power PPL view of plagioclase grain (outlined) seeded with numerous small clinozoisite/epidote grains reflecting static greenschist facies retrogression. d) PPL view of intergrown aggregates of fine grained colourless amphibole, quartz, chlorite and calcite (all after pyroxene – location of relict grain outlined) with rim of yellow epidote. e) PPL view of fine quartz-epidote veins (labelled) overprinted by white mica-chlorite phyllonitic fabric (highlighted in yellow), with feldspar clasts showing fibrous pressure shadows. f) Hand specimen sample of gneiss and quartz-epidote veins (labelled) in basal Devonian Clair Group.

Figure 6) Selected minerals and microstructures from the samples analysed using U-Pb zircon geochronology. a) PPL view of sheared granitic gneiss with brown foliation-parallel pseudotachylyte with tensile offshoot suggesting top to the left sense of shear (from BGS thin section collection). b) Cross polar view of granodioritic-dioritic gneiss showing intergrown altered plagioclase, pyroxene, amphibole and secondary blue birefringent chlorite (dated sample HM11686). c) Cross polar view of marginal myrmekite (myrm) development in granitic gneiss, with weak subgrain development in quartz (dated sample HM11691). d) Cross polar view of granodioritic gneiss showing localised retrogression and breakdown of plagioclase to fine grained aligned aggregates of white mica and epidote, marginal subgrain rotation recrystallization in quartz and fibrous quartz-white mica tails

(labelled) around feldspars (dated sample HM11692). e) PPL view of granodioritic gneiss showing fine aggregates of green amphibole, biotite and epidote, possibly after orthopyroxene (relict grain outlined) intergrown with plagioclase, quartz and a dark relict grain of altered clinopyroxene (CPx) (dated sample HM11699). f) PPL view of more mafic granitic gneiss showing intergrown plagioclase and brown partially altered pyroxene with prominent ore-rich alteration rims (dated sample HM11700).

Figure 7) Selected CL images of zircons from basement gneisses from the Sula Sgeir-Orkney, Lancaster, Greater Clair and Victory sub-areas. Spot size is 30 μm. A) HM11705: BGS borehole 88/02, analysis 106. B) HM11705: BGS borehole 88/02, analysis 107. C) HM11686: well 204/25-1, analysis 094. D) HM11688: well 204/27-1, analyses 022 and 023. E) HM11691: well 205/20-1, analyses 050 and 051. F) HM11691: well 205/20-1, analyses 063 and 064. G) HM22702: well 206/12-1, analysis 277. H) HM11698: well 208/23-1, analyses 012 and 013. I) HM11699: well 208/26-1, analysis 064. J) HM11699: well 208/26-1, analysis 050 and 051.

Figure 8) U-Pb isotopic compositions of zircons from the Sula Sgeir-Orkney sub-area displayed on Wetherill concordia diagrams, together with best estimates for zircon crystallisation ages. All data-point error ellipses are 2σ. A) Granitic gneiss, HM11705, BGS borehole 88/02, 13.00 m (all data); B) Granodioritic gneiss, HM11709, BGS shallow borehole 59-04/85DM (all data); C) Granodioritic gneiss, HM11709, BGS shallow borehole 59-04/85DM (showing zircons used for concordia age determination); D) Granite, HM11711, BGS shallow borehole 59-04/186DM (all data); E) Granite, HM11711, BGS shallow borehole 59-04/186DM (showing zircons used for concordia age determination).

Figure 9) U-Pb isotopic compositions of zircons from the Lancaster sub-area displayed on Wetherill concordia diagrams, together with best estimates for zircon crystallisation ages. All data-point error ellipses are 2σ. A) Granodioritic-tonalitic gneiss, HM11686, well 204/25-1, 2870.43 m (all data); B) Granodioritic-tonalitic gneiss, HM11686, well 204/25-1, 2870.43 m (showing data used for upper intercept age determination); C) Granodioritic gneiss, HM11687, 204/26-1A, well 2648.68 m (all data); D) Granodioritic gneiss, HM11687, 204/26-1A, well 2648.68 m (showing data used for upper intercept age determination); E) Granodioritic gneiss, HM11687, 204/26-1A, well 2648.68 m (showing data used for concordia age determination); F) HM11688, well 204/27-1, 2136.20 m (all data); G) HM11688, well 204/27-1, 2136.20 m (showing data used for upper intercept age determination); H) Granite, HM11688, well 204/27-1, 2136.20 m (showing data used for concordia age determination); I) Granodioritic gneiss, HM11689, well 204/28-1, 1941.55 m (showing all data and determination of upper intercept age); J) Granodioritic gneiss, HM11689, well 204/28-1, 1941.55 m (showing data used for concordia age determination).

Figure 10) U-Pb isotopic compositions of zircons from the Greater Clair and Victory sub-areas displayed on Wetherill concordia diagrams, together with best estimates for zircon crystallisation ages. All data-point error ellipses are 2σ.

Greater Clair: A) Granitic gneiss, HM11691, 205/20-1, 2017.50 m m (showing all data and determination of upper intercept age); B) Granodioritic gneiss, HM11692, 206/7a-2, 2141.40 m (all data); C) Granodioritic gneiss, HM11692, 206/7a-2, 2141.40 m (showing data used for concordia age determination); D) Granodioritic gneiss, HM11694, 206/7a-2, 2593.30 m (all data); E) Granodioritic

gneiss, HM11694, 206/7a-2, 2593.30 m (showing data used for upper intercept age determination); F) Granodioritic gneiss, HM22702, 206/12-1, 1716.63 m (showing all data and determination of upper intercept age).

Victory: G) Granitic gneiss, HM11698, 208/23-1, 2071.26 m (showing all data and determination of upper intercept age); H) Granodioritic gneiss, HM11699, 208/26-1, 3741.31 m (all data); I) Mafic-granitic gneiss, HM11700, 208/27-2, 1357.11 m (all data); J) Mafic-granitic gneiss, HM11700, 208/27-2, 1357.11 m (showing data used for concordia age determination).

Figure 11) Probability – density plots for selected samples of basement and cover sequences. Dark grey areas are zircons with <10% discordance, pale grey areas are zircons with >10% discordance. n = number of zircons with <10% discordance in total zircon data set. See Figure 1 for location of wells unless indicated otherwise. A) Granodioritic basement gneiss sample HM11699, Victory sub-area (208/26-1, 3741.31 m), 23 zircons with 99-101% concordance; B) Upper Jurassic Rona Member sandstone sample HM12189, Lancaster sub-area (204/27-1, 2094.65 m), n = 89/106. No zircons <2500 Ma detected. C) Upper Jurassic Rona Member sandstone sample HM12194, Lancaster sub-area (202/3-1A, 1642.50 m), n = 55/89. Spectrum also includes six younger zircons with <10% discordance at 494 Ma, 1014 Ma, 1353 Ma, 1551 Ma, 1960 Ma and 2127 Ma. D) Lower Cretaceous Royal Sovereign Formation sample HM12357, Greater Clair sub-area (206/4-1, 4115 m), n=84/99. Spectrum also includes one younger zircon with <10% discordance at 1692 Ma. E) Triassic sandstone sample HM12172, Victory sub-area (213/23-1, 3598.36 m), n=54/107. Spectrum also includes two younger zircons with <10% discordance at 1096 Ma and 1751 Ma. F) Lower Cretaceous (Albian) sample W4629, Kangerlussuaq, East Greenland, n=34/53. See Figure 15 for location. Data from Whitham et al. (2004), acquired by SHRIMP.

Figure 12) Hf isotope data displayed in the εHf(t) versus U-Pb age diagram. Symbols represent analyses of individual growth domains of zircon from the different samples. The depleted mantle (Chauvel et al. 2008) and the fields of the Neoarchaean to Palaeoarchaean crust, assuming a crustal $^{176}Lu/^{177}Hf$ of 0.0113, are shown for comparison.

Figure 13) Map based on Fig. 1 showing geographic distribution of U-Pb zircon and Hf T_{DM} ages from the basement gneisses, offshore west of Shetland (current study) and from Ritchie et al. (2011).

Figure 14) Probability – density plot of all zircon ages with <5% discordance from crystalline basement west of Shetland (n=313), showing the dominance of crystallisation ages between ca 2720 Ma and 2750 Ma, with a subordinate older group between ca 2790 Ma and 2840 Ma.

Figure 15) Simplified map showing the major age provinces within the British Isles, Ireland and Greenland, showing suggested location and extent of FST and its approximate southern boundary. MTZ = Moine Thrust Zone; WBF = Walls Boundary Fault; GGFZ = Great Glen Fault Zone; Nag = Nagssugtoqidian; CGC = Central Greenland (Rae) Craton; KB = Kangerlussuaq Basin; EGC = East Greenland Caledonides. RT = Rhiconich Terrane of Lewisian Gneiss Complex

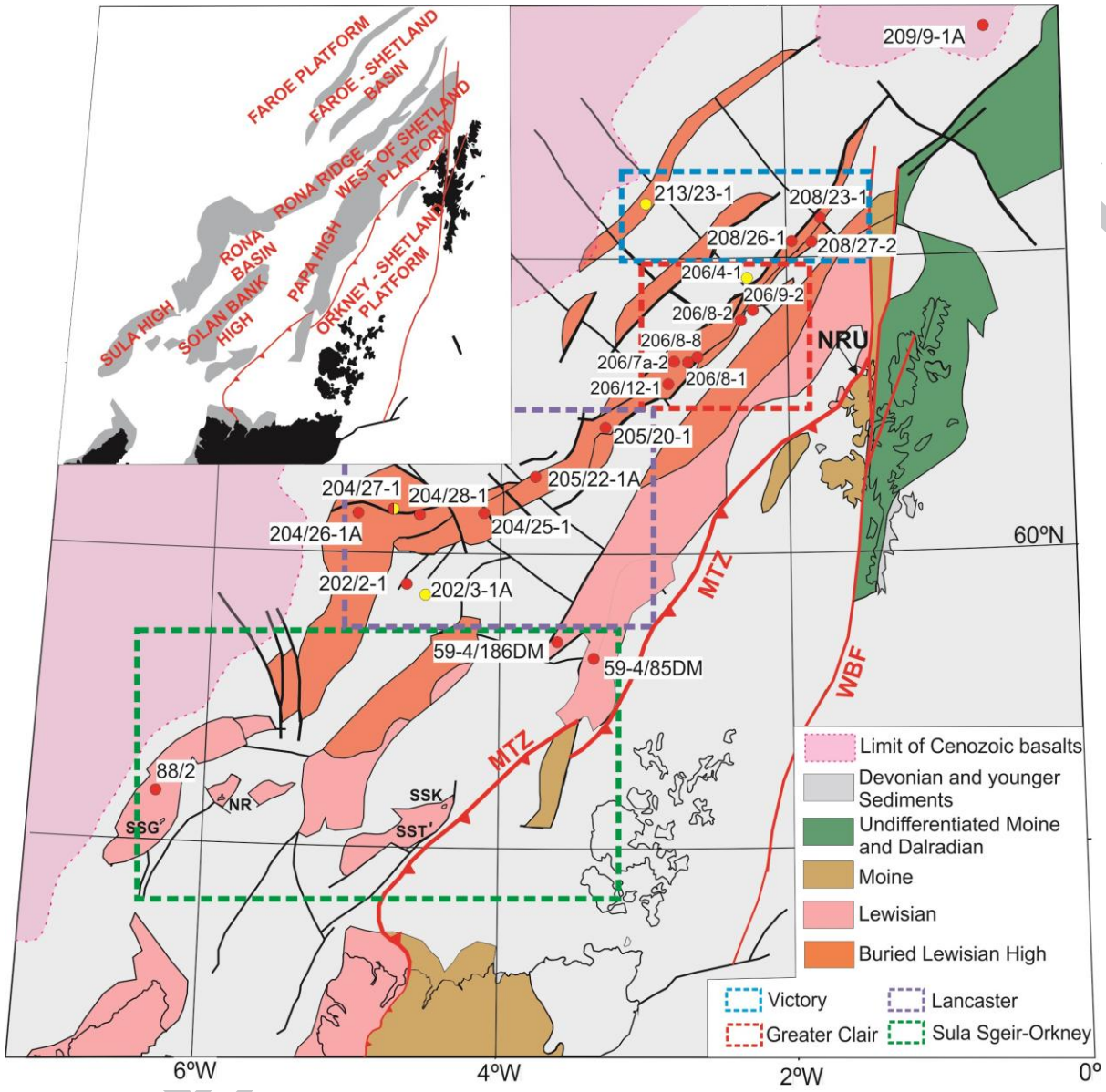

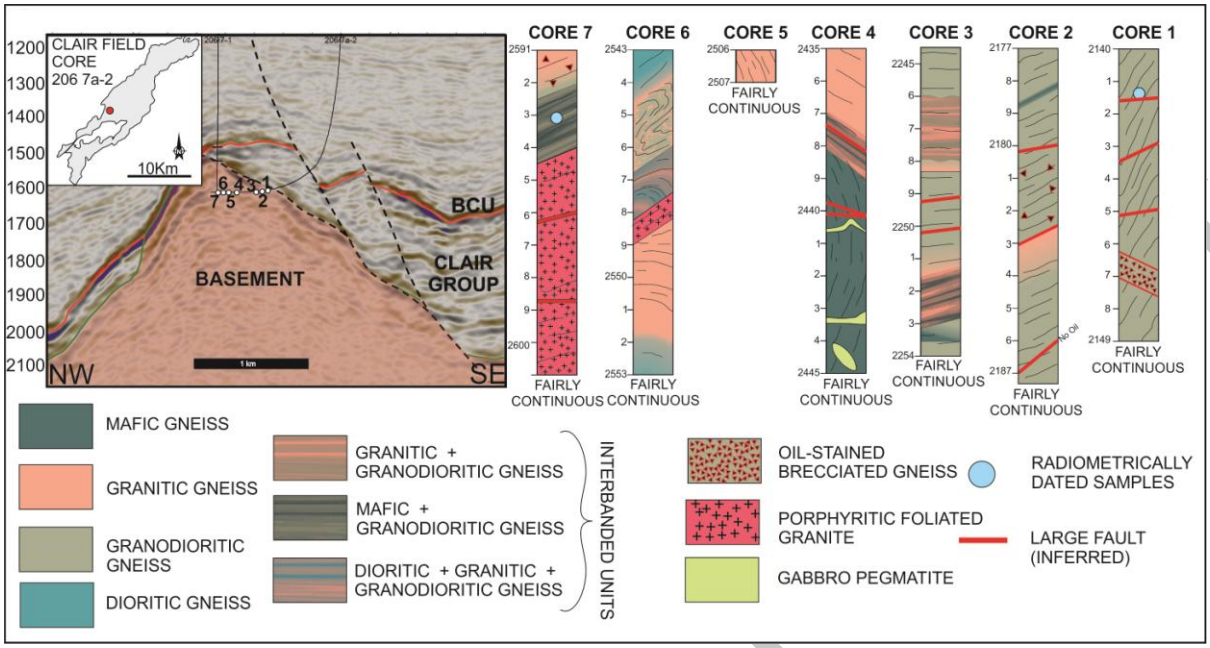

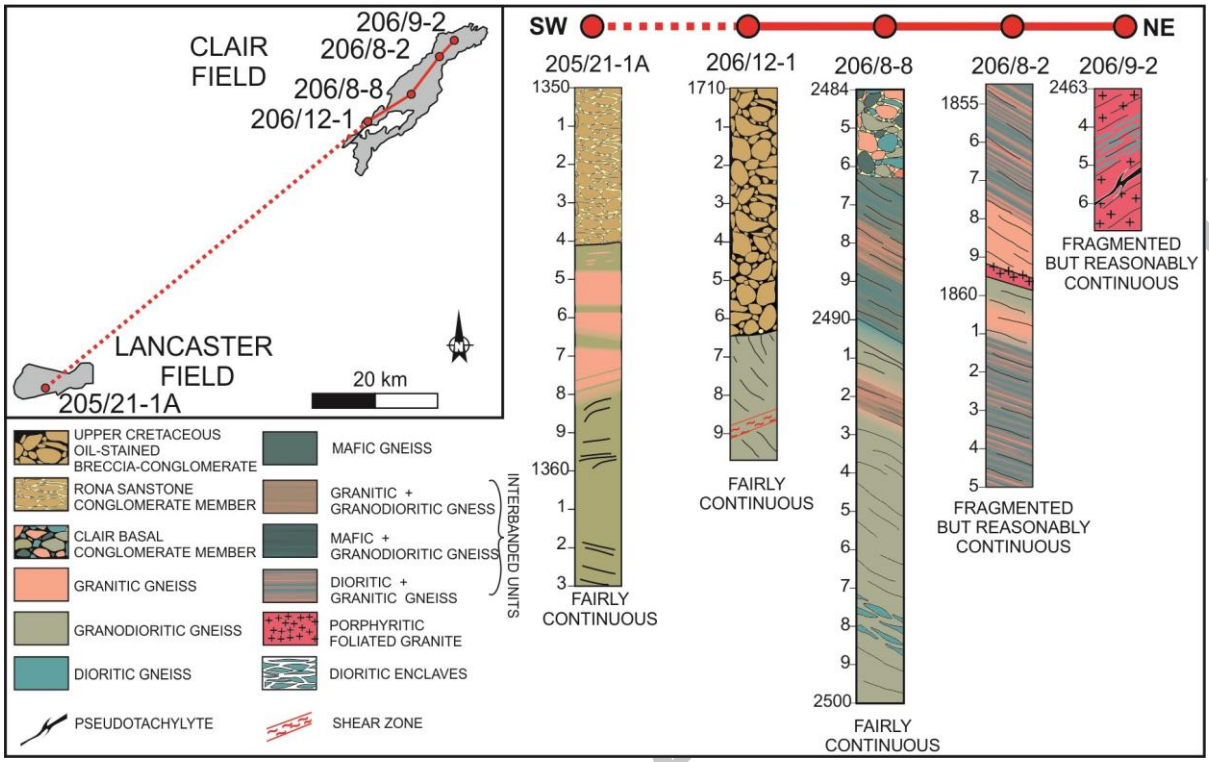

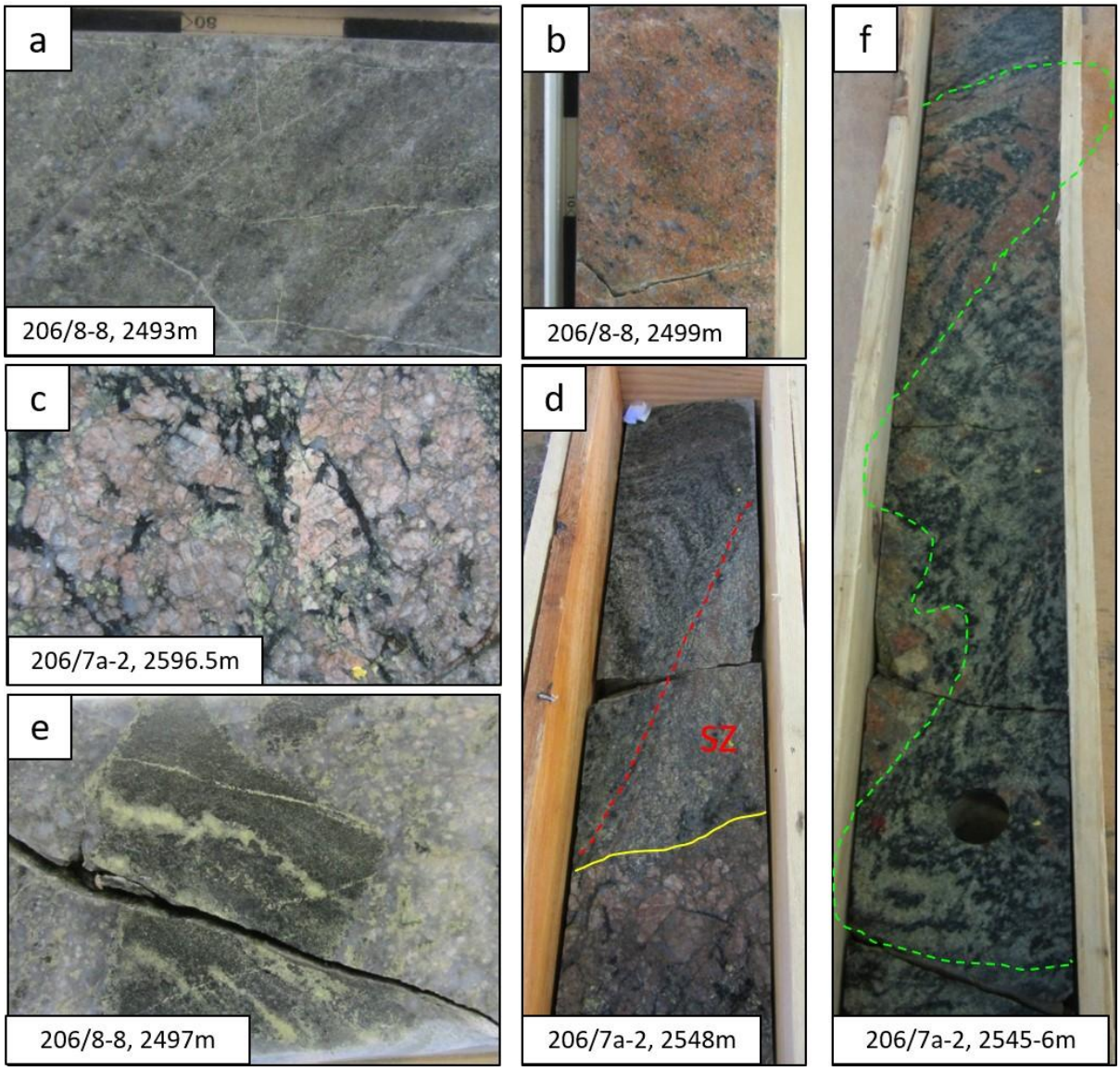

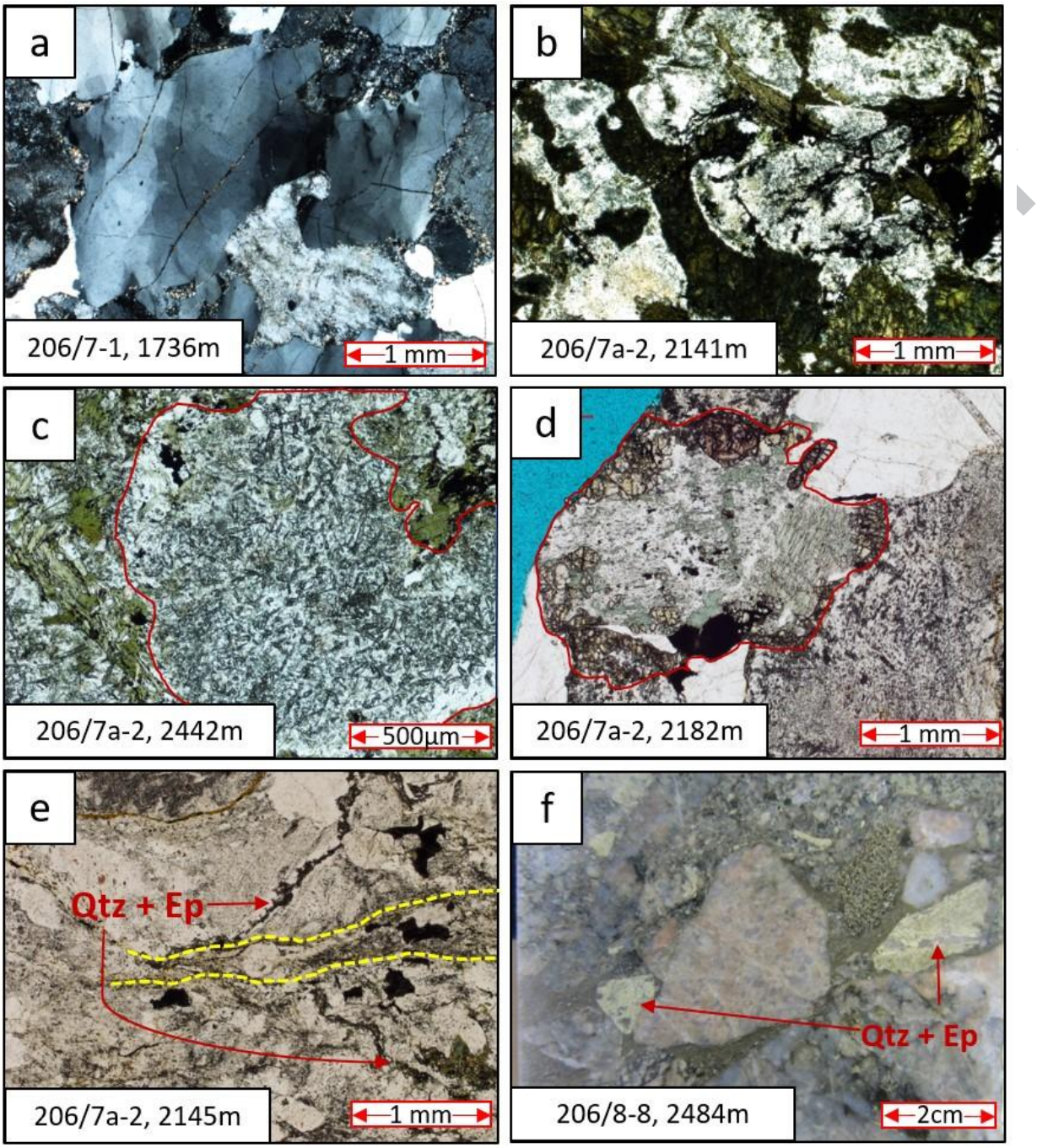

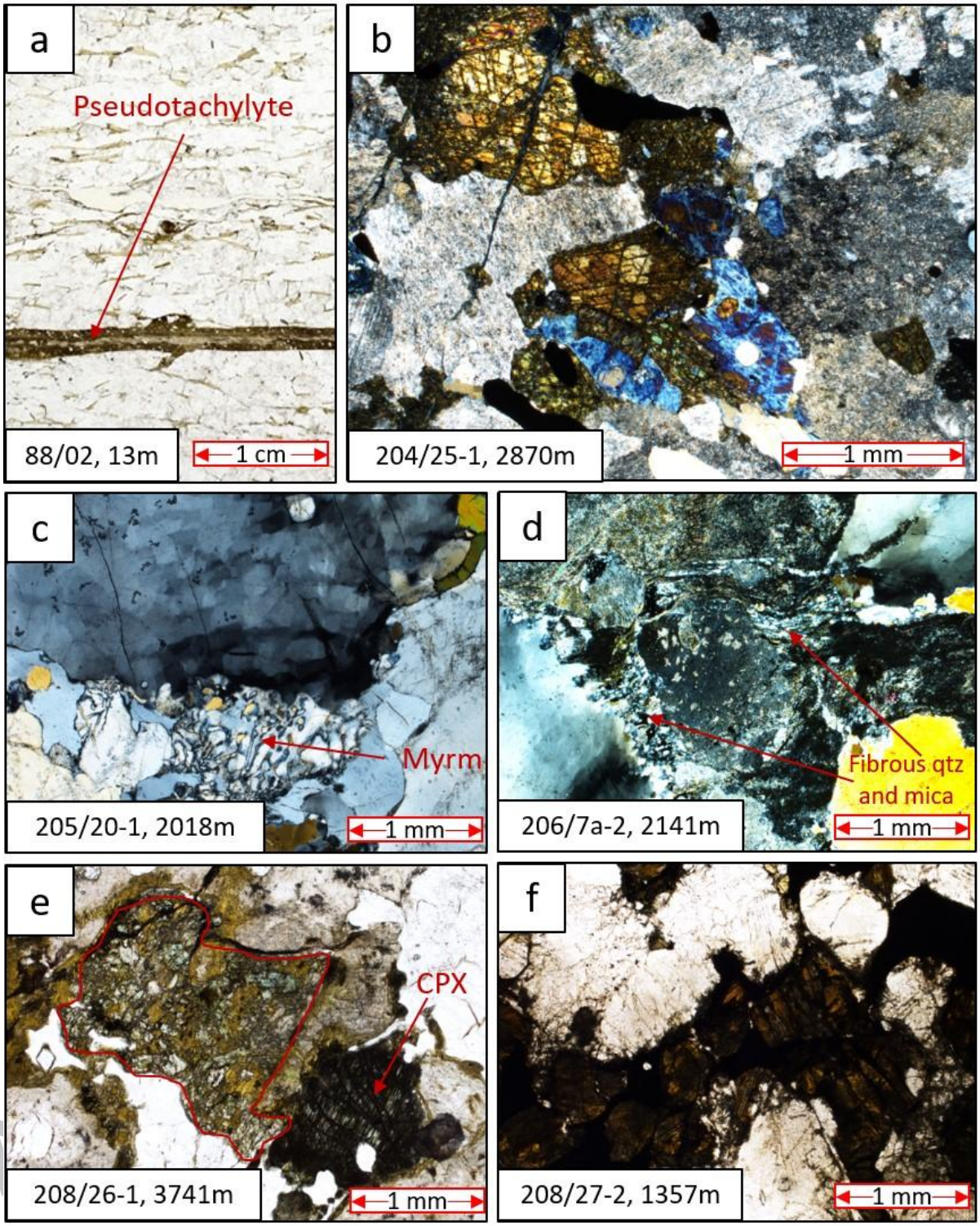

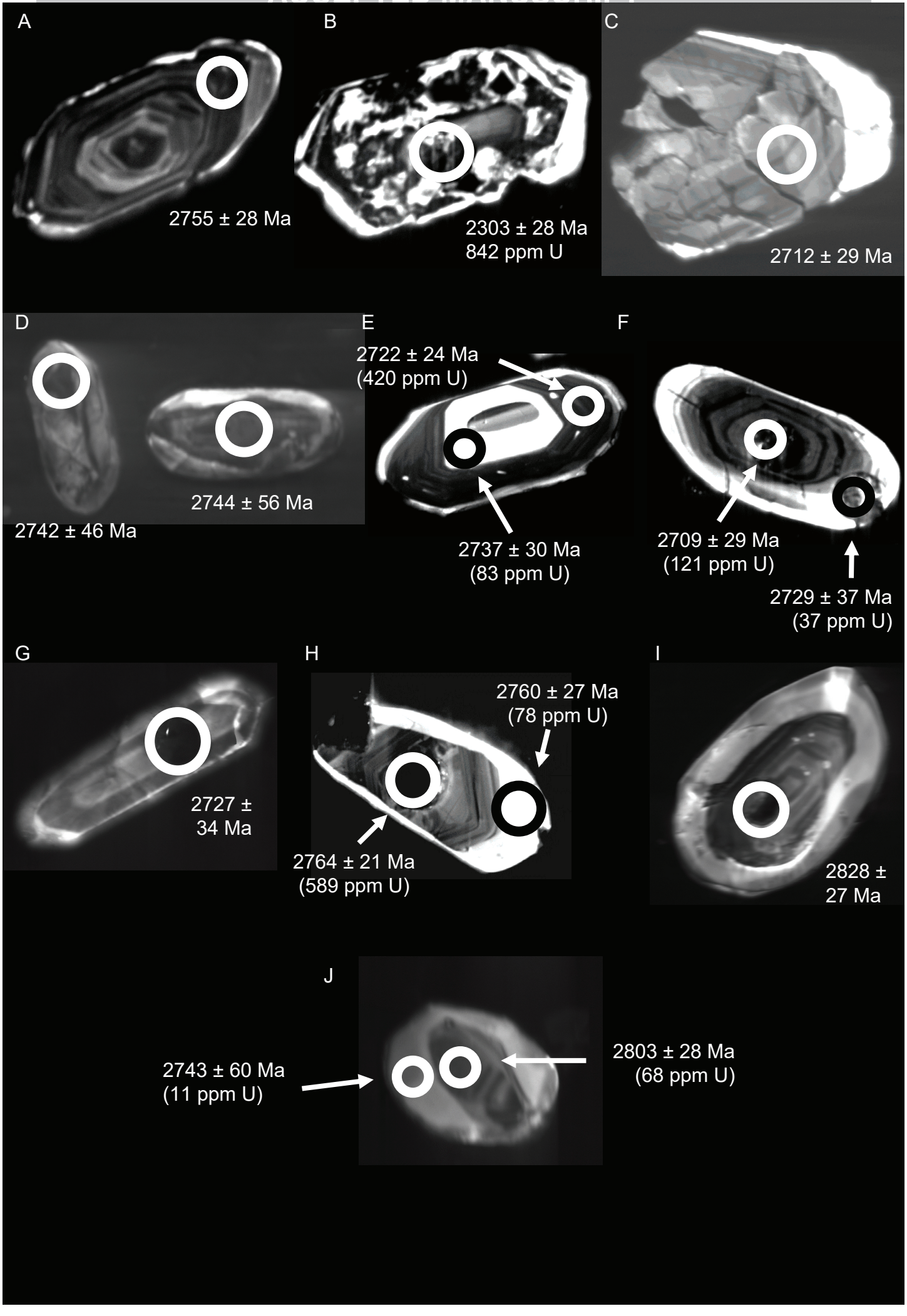

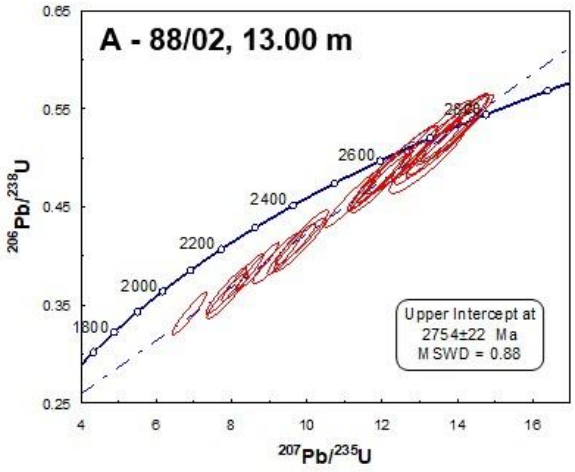

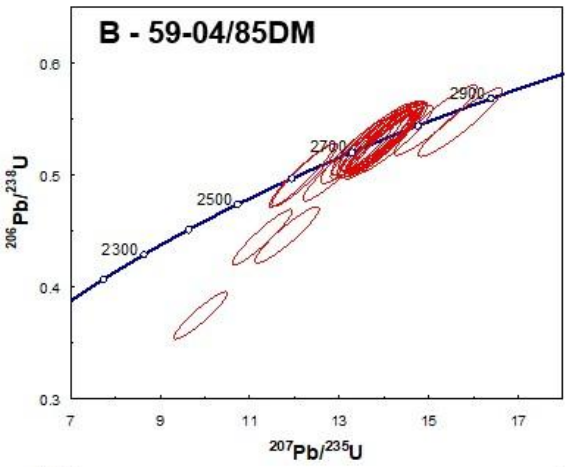

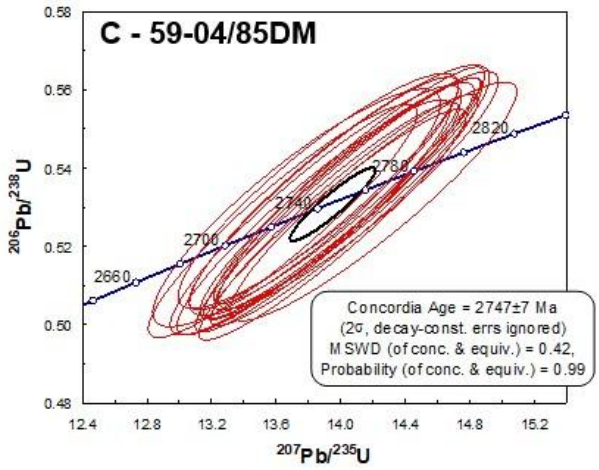

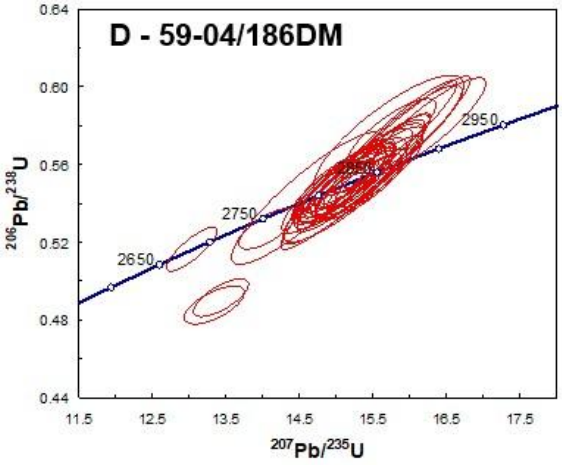

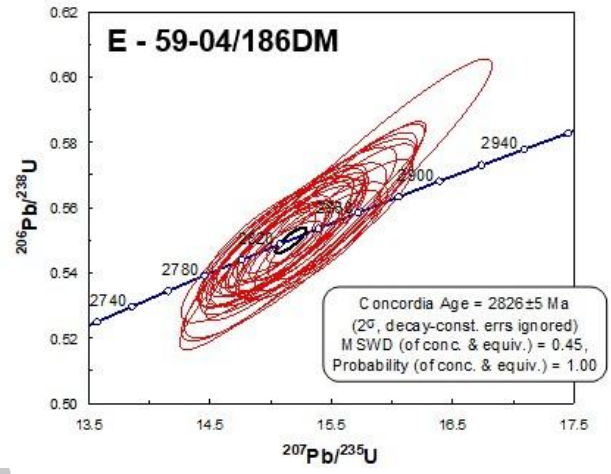

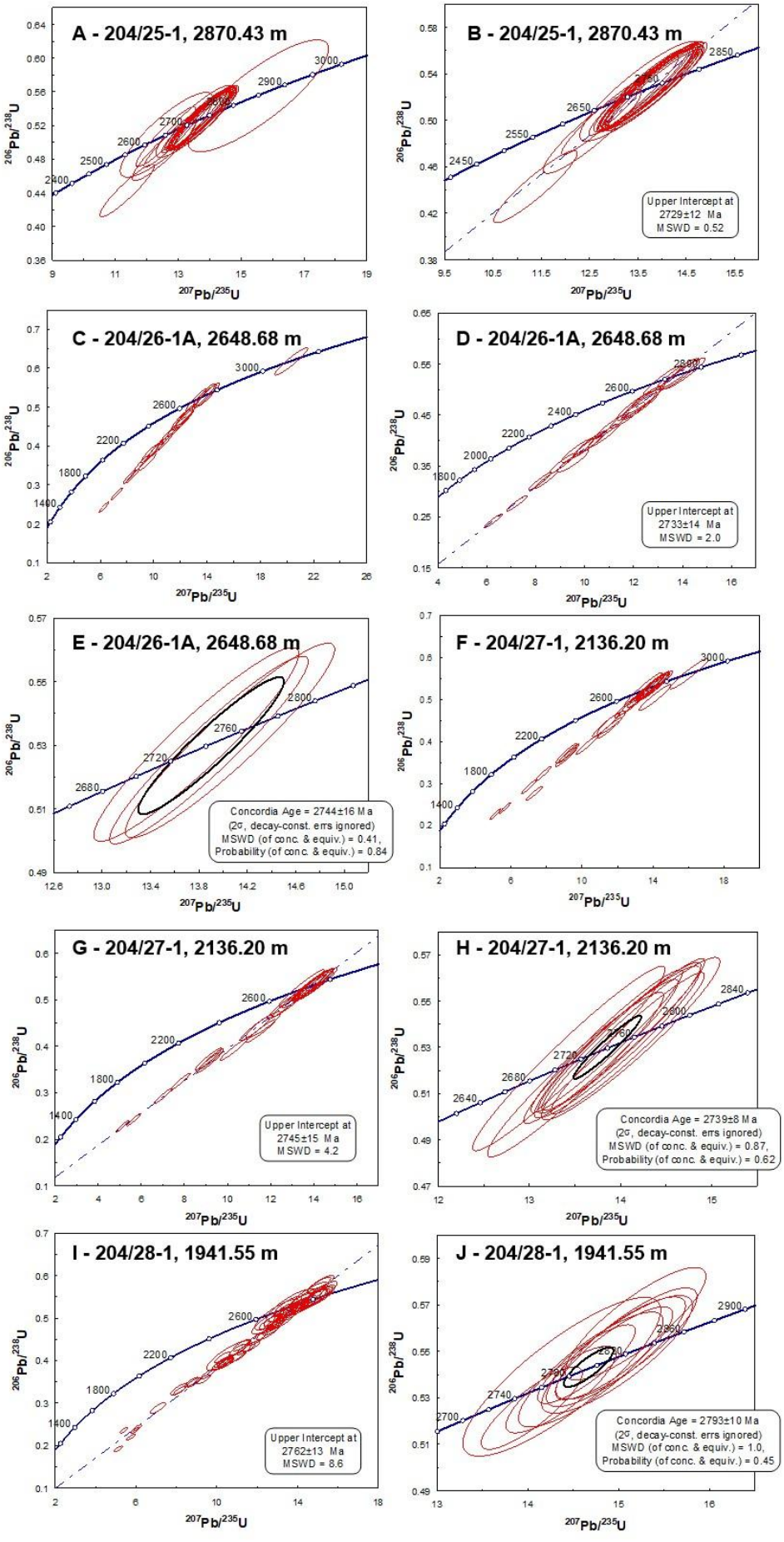

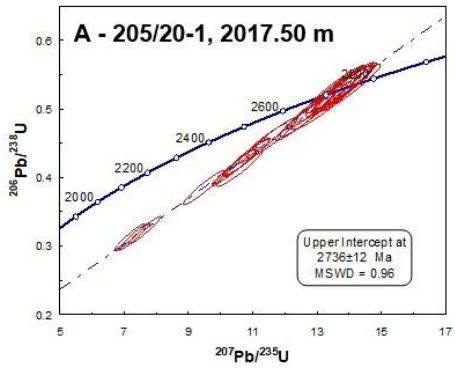

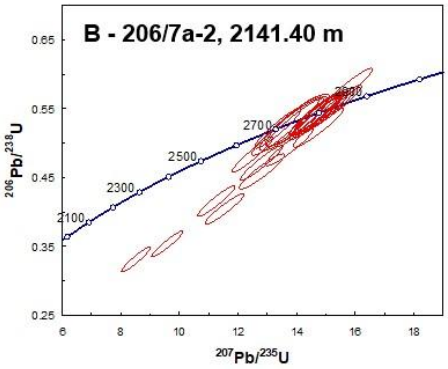

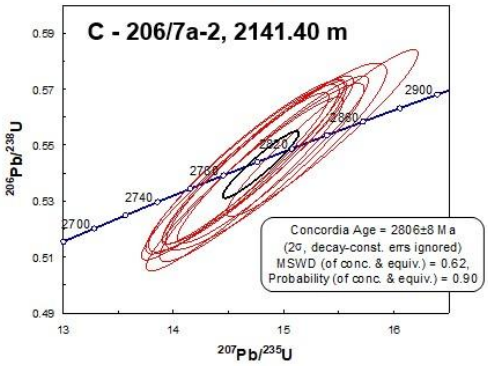

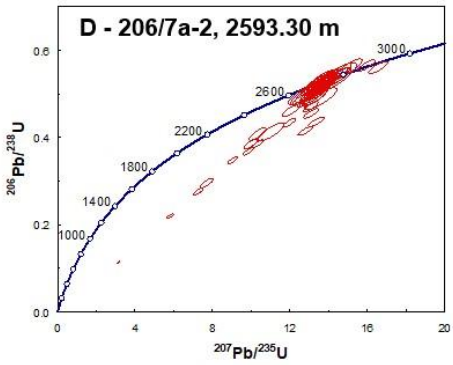

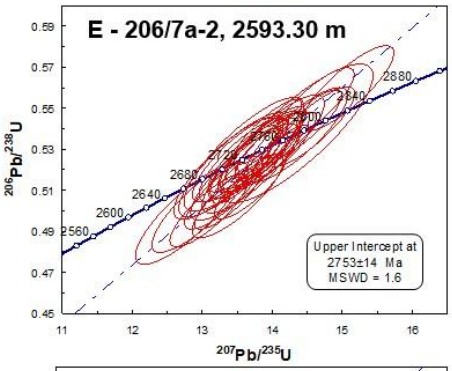

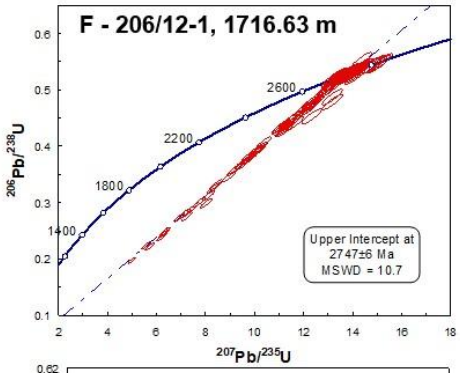

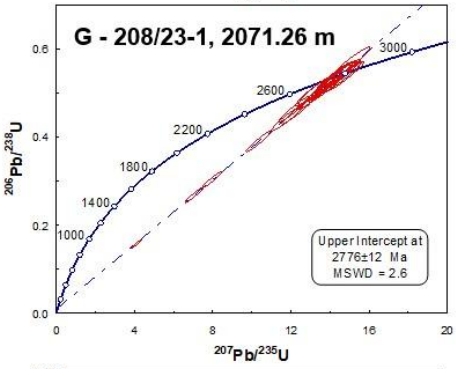

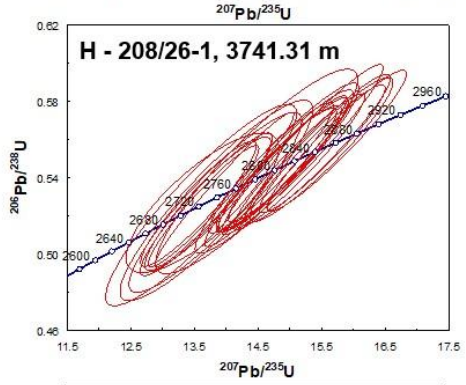

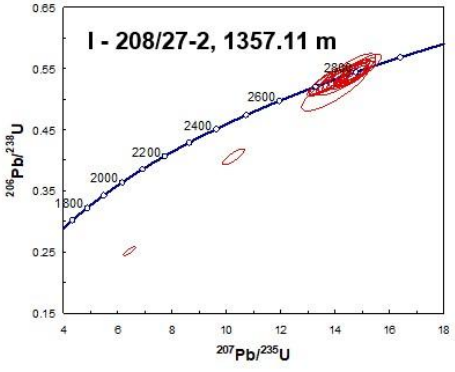

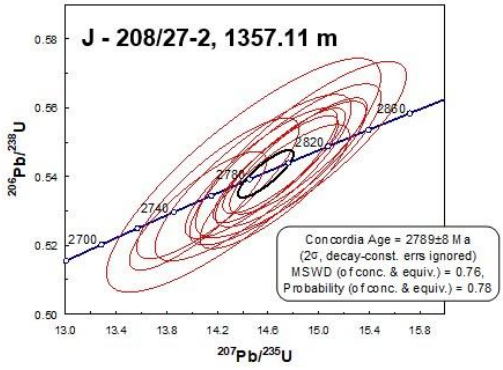

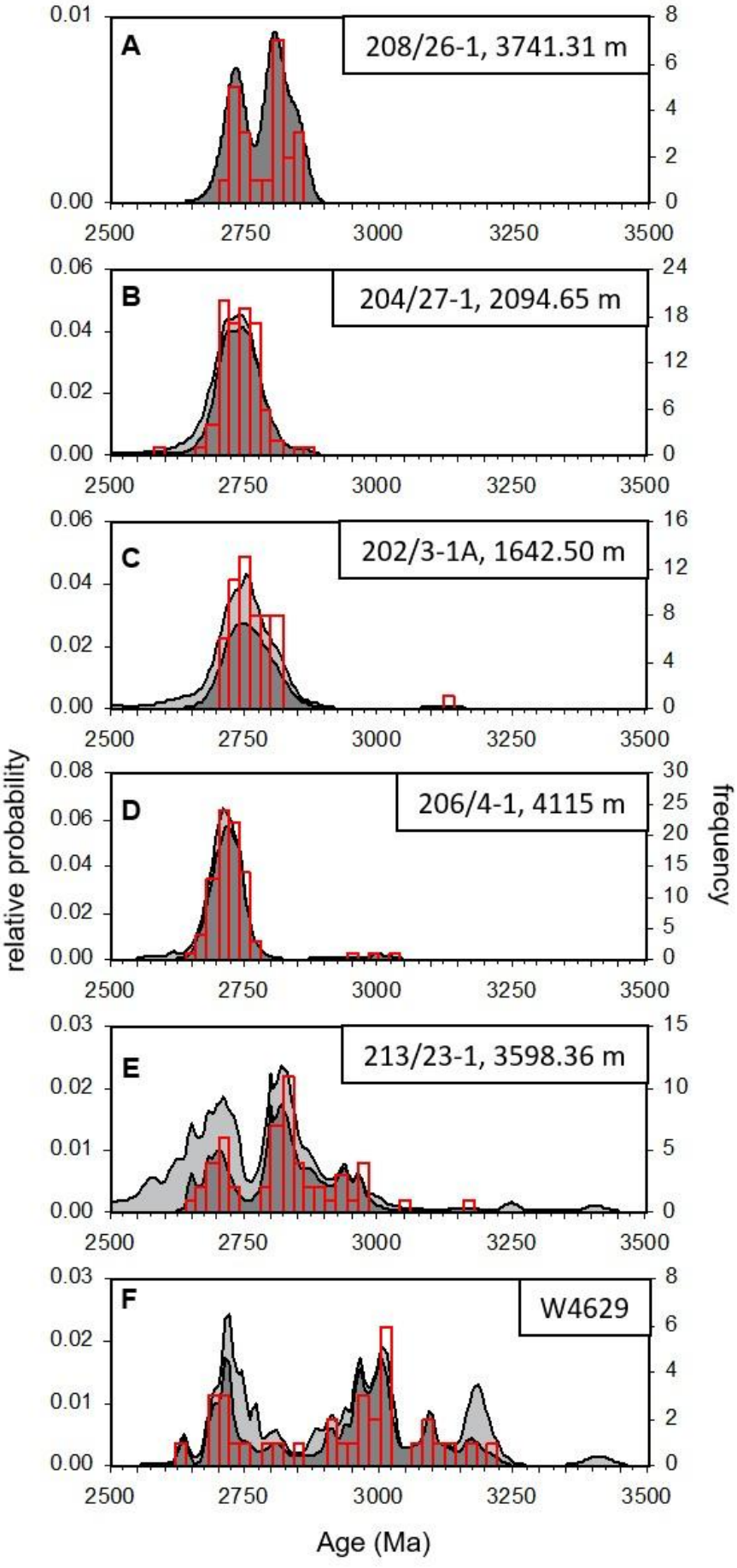

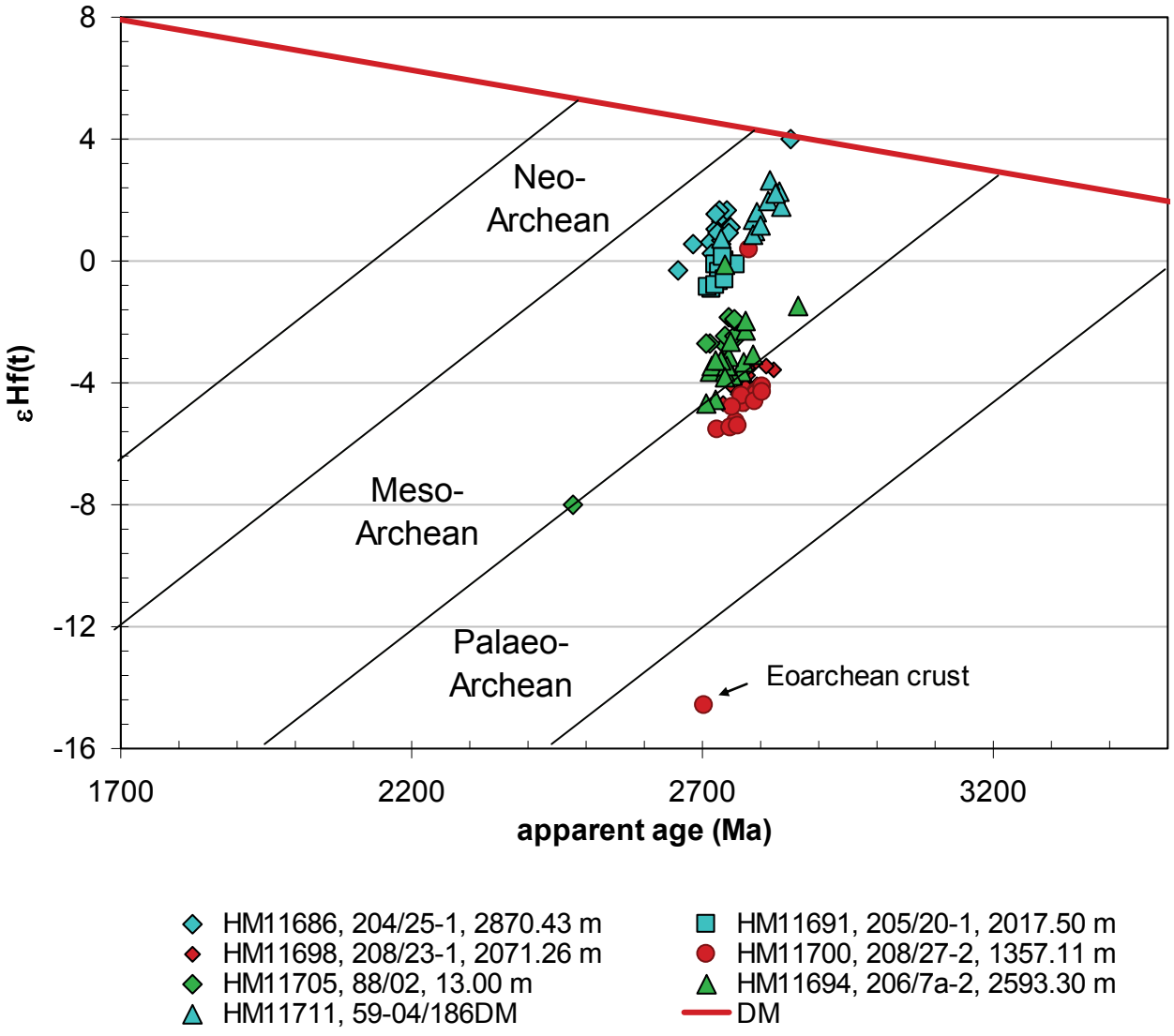

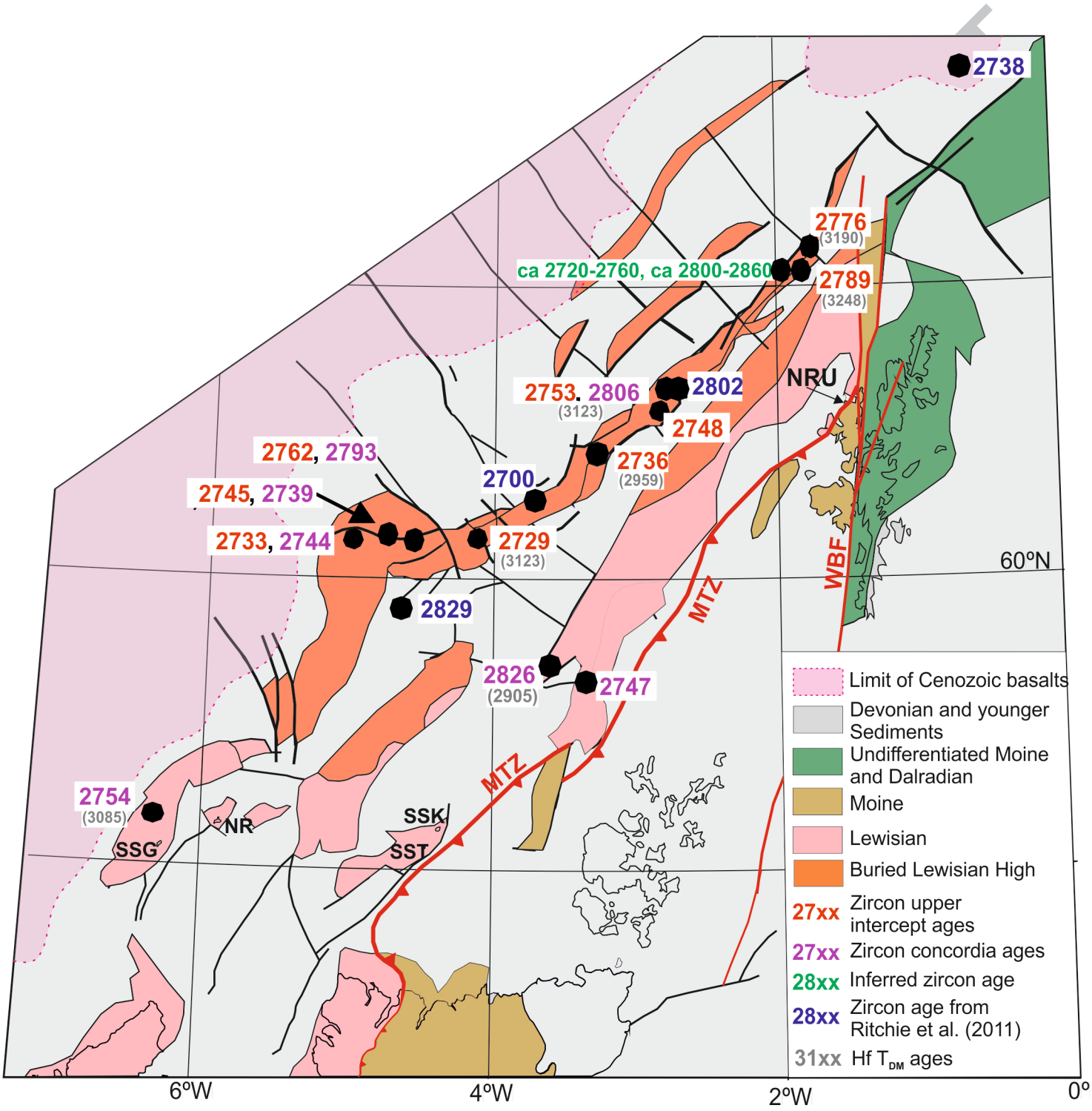

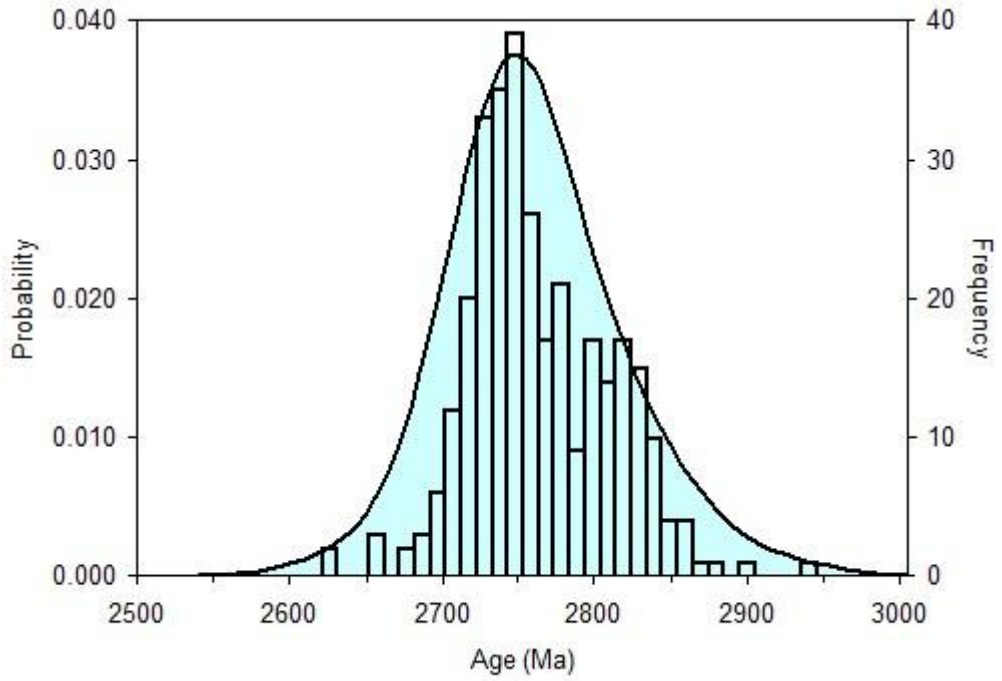

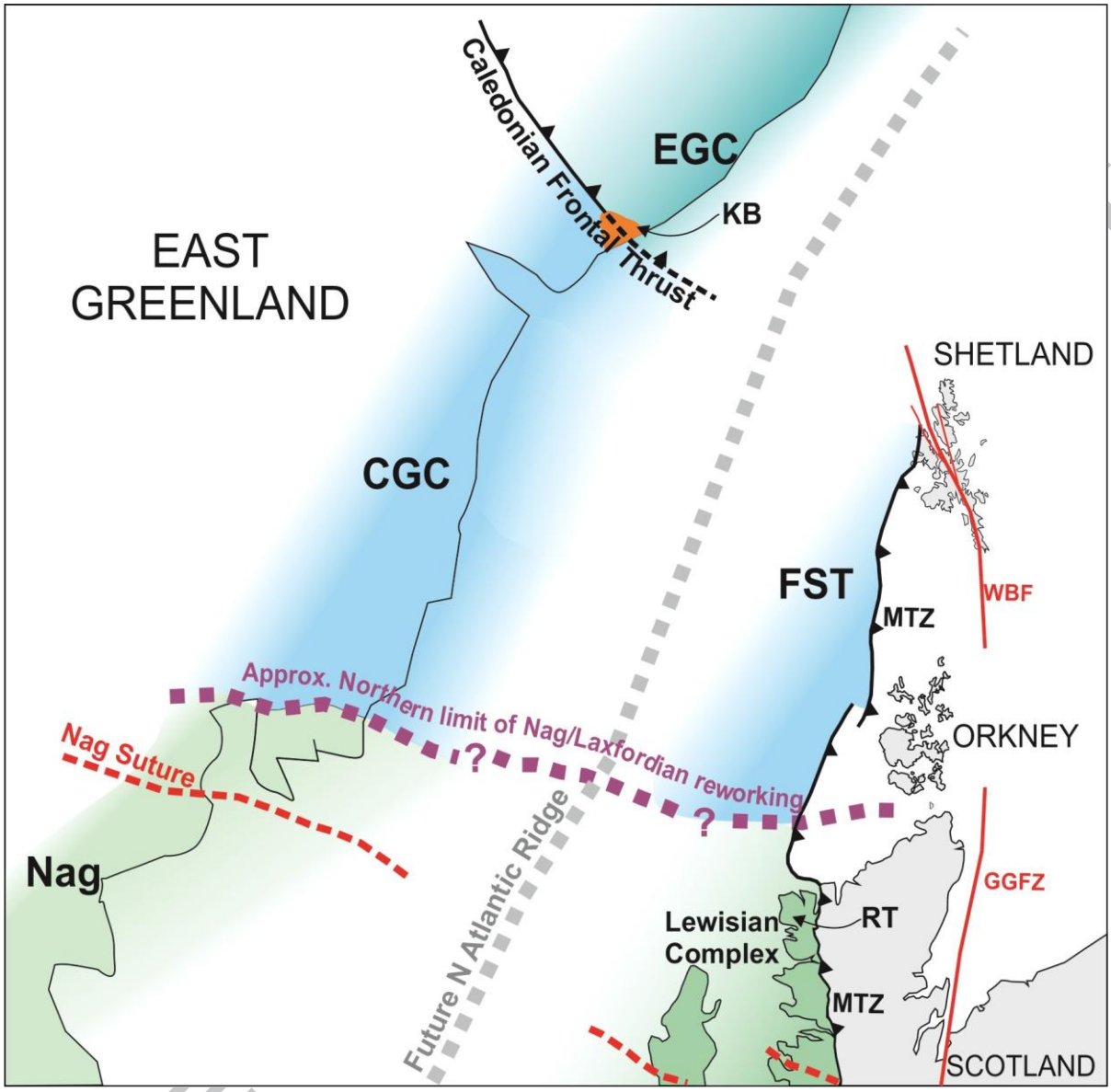

Highlights

Orthogneisses dominate basement rocks that underlie the Faroe-Shetland Basin (FSB)

U-Pb zircon analyses yield narrow range of Neoarchean protolith ages (ca 2.7-2.8 Ga)

Detrital zircon data from FSB cover sequences yield similar range of source ages

Faroe-Shetland Terrane lies in N foreland of the Nagssugtoqidian-Laxfordian orogen

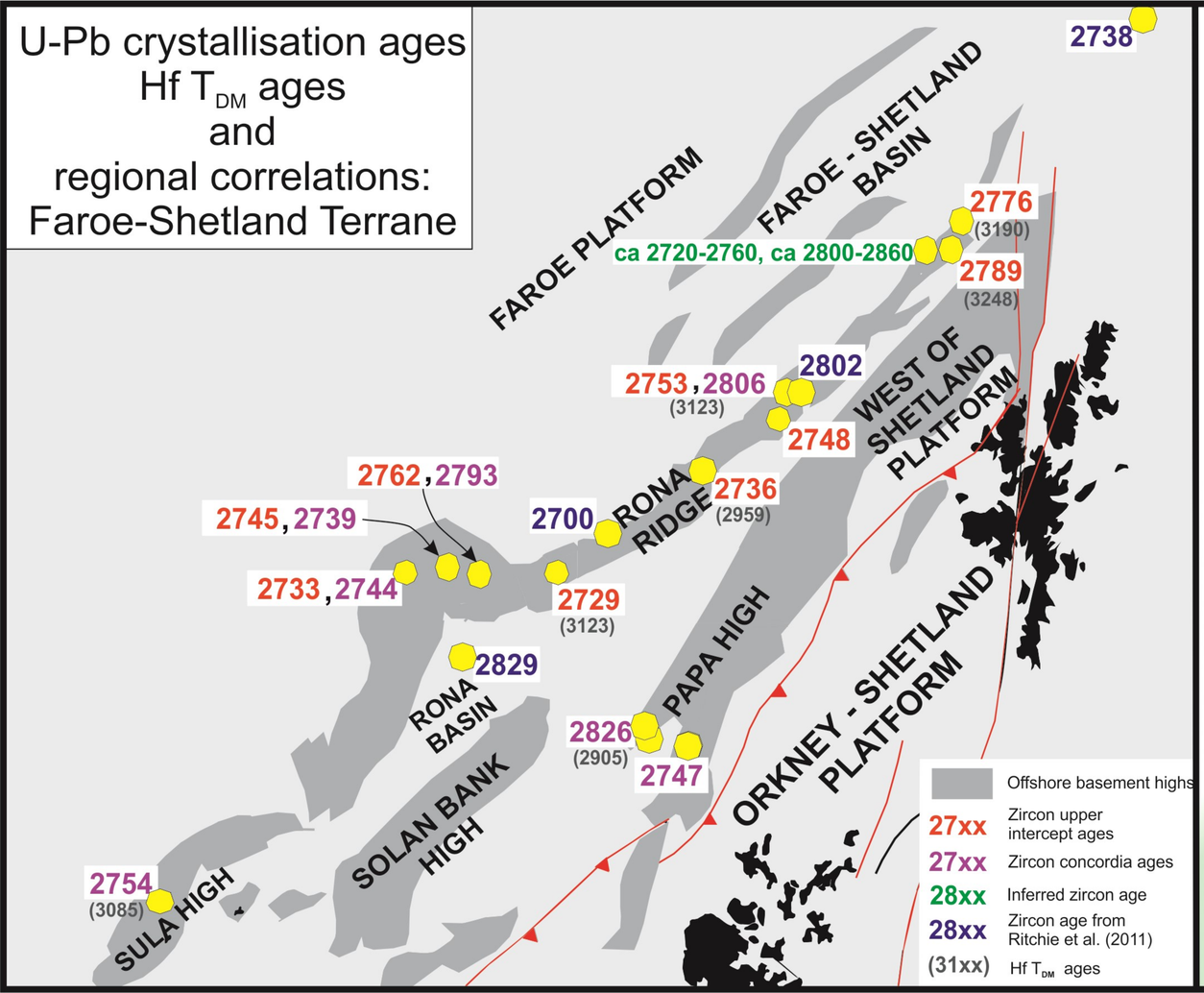
U-Pb crystallisation ages
Hf T_{DM} ages
and
regional correlations:
Faroe-Shetland Terrane
2738
FAROE PLATFORM
FAROE - SHETLAND BASIN
2776
(3190)
ca 2720-2760, ca 2800-2860
2789
(3248)
2753, 2806
(3123)
2802
2748
WEST OF SHETLAND PLATFORM
2762, 2793
2745, 2739
2700
RONA RIDGE
2736
(2959)
2733, 2744
2729
(3123)
2829
RONA BASIN
PAPA HIGH
2826
(2905)
2747
ORKNEY - SHETLAND PLATFORM
SOLAN BANK HIGH
2754
(3085)
SULA HIGH
Offshore basement highs
27xx Zircon upper intercept ages
27xx Zircon concordia ages
28xx Inferred zircon age
28xx Zircon age from Ritchie et al. (2011)
(31xx) Hf T_{DM} ages

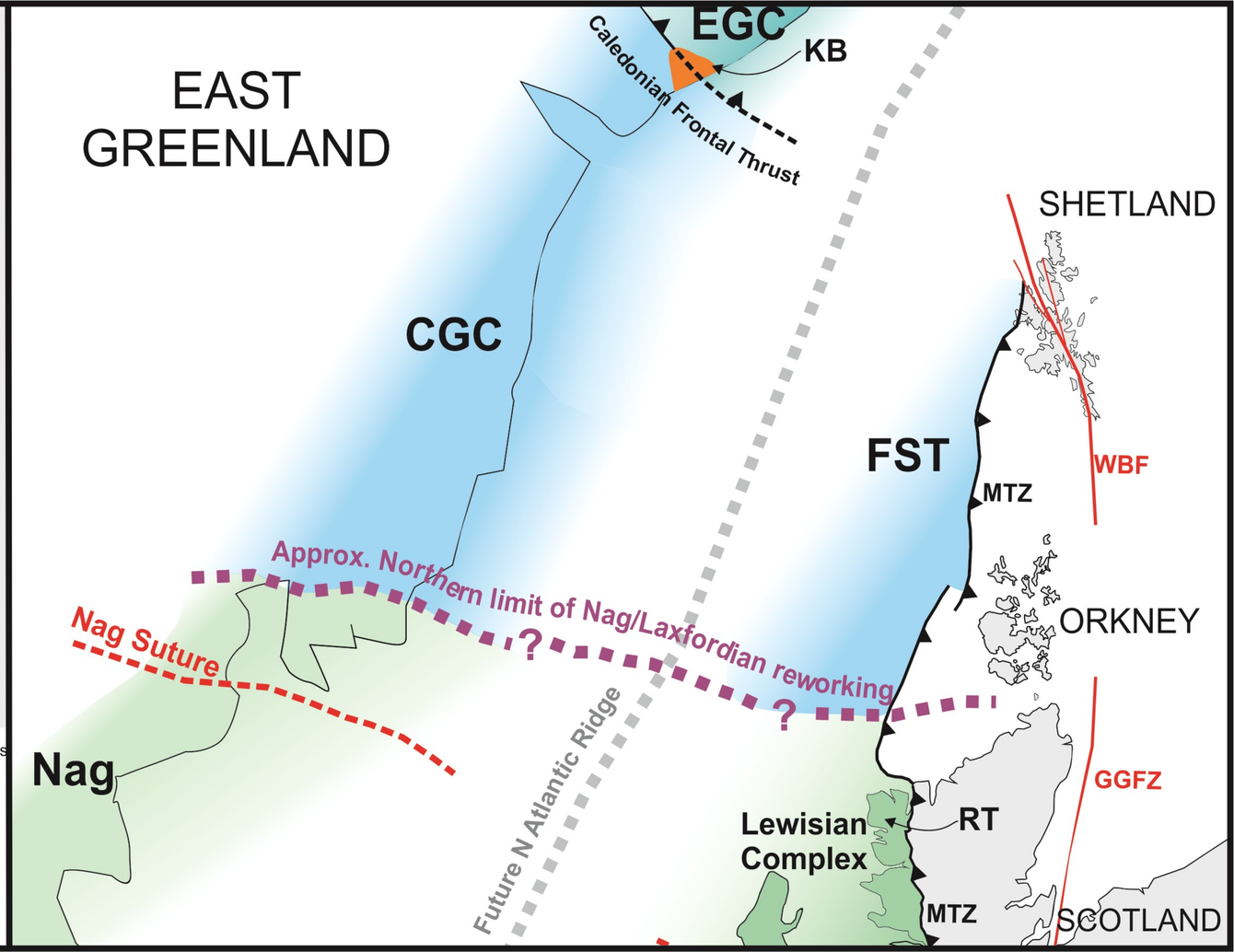
EAST GREENLAND
EGC
KB
Caledonian Frontal Thrust
SHETLAND
CGC
FST
WBF
MTZ
Approx. Northern limit of Nag/Laxfordian reworking
?
?
ORKNEY
Nag Suture
Nag
Future N Atlantic Ridge
GGFZ
Lewisian Complex
RT
MTZ
SCOTLAND